

# Best Experienced Payoff Dynamics and Cooperation in the Centipede Game: Online Appendix

William H. Sandholm\*, Segismundo S. Izquierdo<sup>†</sup>, and Luis R. Izquierdo<sup>‡</sup>

December 4, 2018

## Contents

<b>I</b>	<b>Exact and numerical calculation in <i>Mathematica</i></b>	<b>2</b>
I.1	Algebraic numbers and solutions to polynomial equations . . . . .	2
I.2	Algorithms from computational algebra . . . . .	3
I.3	Numerical evaluation and precision tracking . . . . .	3
<b>II</b>	<b>The <code>BEP_Centipede.nb</code> notebook</b>	<b>4</b>
II.1	Exact analysis . . . . .	4
II.2	Numerical analysis . . . . .	5
II.3	More on computation of approximate rest points and eigenvalues . . . . .	6
<b>III</b>	<b>Dimension reduction for local stability analysis</b>	<b>8</b>
<b>IV</b>	<b>Repulsion from the backward induction state under test-adjacent</b>	<b>10</b>
IV.1	Test-adjacent, min-if-tie . . . . .	10
IV.2	Test-adjacent, stick-if-tie: . . . . .	12
<b>V</b>	<b>Approximate components of attractor <math>\xi^*</math> of <math>\text{BEP}(\tau, 1, \beta)</math> dynamics</b>	<b>13</b>
V.1	Test-all . . . . .	14
V.2	Test-two . . . . .	18
V.3	Test-adjacent . . . . .	22
<b>VI</b>	<b>Approximate eigenvalues of <math>DV(\xi^*)</math> for <math>\text{BEP}(\tau, 1, \beta)</math> dynamics</b>	<b>26</b>
VI.1	Test-all . . . . .	26
VI.2	Test-two . . . . .	28

---

\*Department of Economics, University of Wisconsin.

<sup>†</sup>Department of Industrial Organization, Universidad de Valladolid.

<sup>‡</sup>Department of Civil Engineering, Universidad de Burgos.

VI.3	Test-adjacent . . . . .	30
VII	Estimates of the basin of attraction of $\xi^+$ for $\text{BEP}(\tau^{\text{all}}, \kappa, \beta^{\text{min}})$ dynamics in Centipede of length $d = 4$	33
VIII	Saddle points of $\text{BEP}(\tau^{\text{all}}, \kappa, \beta^{\text{min}})$ dynamics in Centipede of length $d = 4$	36
IX	General formulation of best experienced payoff dynamics	36
X	Multinomial formulas for best experienced payoff dynamics	37
XI	Formulas for $\text{BEP}(\tau, 1, \beta)$ dynamics in Centipede	39
	XI.1 Test-all . . . . .	39
	XI.2 Test-two . . . . .	41
	XI.3 Test-adjacent . . . . .	42

## I. Exact and numerical calculation in *Mathematica*

In this section we describe the built-in *Mathematica* functions we use to prove exact (analytical) results and to obtain numerical evaluations of exact expressions.

### I.1 Algebraic numbers and solutions to polynomial equations

To obtain our analytical results, we take advantage of *Mathematica*'s ability to perform exact computations using algebraic numbers. As described in Strzeboński (1996, 1997), *Mathematica* represents algebraic numbers using `Root` objects, with `Root[poly, k]` designating one of the roots of the minimal polynomial *poly*. The index *k* is used to single out a particular root of *poly*, with the lowest indices referring to the real roots of *poly* in increasing order, and the higher indices referring to the complex roots in a more complicated way. `Root` objects also contain a hidden third element that specifies an *isolating set* for the root, meaning a set containing the root of *poly* in question and no others.

The forms of isolating sets depend on whether roots are isolated using arbitrary-precision floating point methods or exact methods. If *Mathematica*'s default settings are used, then roots are isolated using arbitrary-precision floating point methods based on the Jenkins-Traub algorithm (Jenkins (1969), Jenkins and Traub (1970a,b)), the workhorse numerical algorithm for this purpose. While in theory this algorithm always isolates all real and complex roots of *poly* in disjoint disks in the complex plane, flawless implementation of the algorithm is difficult; see Strzeboński (1997, p. 649).

If we instead use the setting

```
SetOptions[Root, ExactRootIsolation->True]
```

then *Mathematica* isolates roots using exact methods—that is, methods that only use rational number calculations. Real roots of polynomials are isolated in disjoint intervals using the Vincent-Akritas-Strzeboński method, which is based on Descartes' rule of signs and a

classic theorem of Vincent; see Akritas et al. (1994) and Akritas (2010). Complex roots are isolated in rectangles using the Collins and Krandick (1992) method.

Exact roots of univariate polynomials (and much else) can be computed using the *Mathematica* function `Reduce`. When computing the exact rest points of BEP dynamics, we apply `Reduce` to the output of the function `GroebnerBasis`, described next.

## I.2 Algorithms from computational algebra

The *Mathematica* function `GroebnerBasis` is an implementation of a proprietary variation of the algorithm of Buchberger (1965, 1970).<sup>1</sup> Choosing the option `Method -> Buchberger` causes *Mathematica* to use the original Buchberger algorithm, which runs considerably more slowly than the default algorithm; however, there was only one case in which the default algorithm produced a Gröbner basis and the Buchberger algorithm failed to terminate.

The *Mathematica* function `CylindricalDecomposition` implements the Collins (1975) cylindrical algebraic decomposition algorithm with various improvements.<sup>2</sup> If this function is run in its default mode, it makes use of arbitrary-precision arithmetic. To force *Mathematica* to work with algebraic numbers, one uses the following settings:

```
SetOptions[Root, ExactRootIsolation->True]
SetSystemOptions["InequalitySolvingOptions" -> "CADDefaultPrecision" -> Infinity]
```

Unfortunately, these settings cause `CylindricalDecomposition` to run extremely slowly, and in the case of BEP dynamics in *Centipede* it only generates a result in two-dimensional cases. Even if arbitrary-precision arithmetic is permitted, the function only generates a result when the dimension is 2 or 3.

## I.3 Numerical evaluation and precision tracking

When *Mathematica* performs calculations using arbitrary-precision numbers  $x$ , it keeps track of the digits whose correctness it views as guaranteed. `Precision[x]` reports the number of correct base 10 significant digits of  $x$ : for instance, if  $x = d_0.d_1d_2d_3d_4\dots \times 10^k$ , the precision is the number of the correct digits in  $d_0.d_1d_2d_3d_4\dots$ . `Accuracy[x]` is the number of correct base 10 digits of  $x$  to the right of the decimal point. Exact numbers in *Mathematica* (e.g., integers, rational numbers, and algebraic numbers) have `Precision` equal to  $\infty$ .

To perform certain parts of our analysis (in particular, checking that an eigenvalue of a derivative matrix has negative real part), we need to numerically evaluate exact numbers and expressions. We do so using the *Mathematica* function `N`. `N[expr, n]` evaluates `expr` as an arbitrary-precision number at guaranteed precision  $n$ . When *Mathematica* performs computations using arbitrary-precision numbers, it maintains precision and accuracy

---

<sup>1</sup>An up-to-date presentation of Gröbner basis algorithms, including many improvements on Buchberger's algorithm, can be found in Cox et al. (2015).

<sup>2</sup>See [reference.wolfram.com/language/tutorial/ComplexPolynomialSystems.html](http://reference.wolfram.com/language/tutorial/ComplexPolynomialSystems.html) for details.

guarantees, the values of which can be accessed using the Precision and Accuracy functions.

While in principle *Mathematica's* precision tracking should not make mistakes, there are at least two reasons for exercising caution when using it in proofs. First, *Mathematica's* precision tracking is not based on *interval arithmetic*, which represents real and complex numbers using exact intervals (in  $\mathbb{R}$ ) and rectangles (in  $\mathbb{C}$ ) that contain the numbers in question, and which relies on theorems that define rules for performing arithmetic and other mathematical operations on these intervals and rectangles that maintain containment guarantees (Alefeld and Herzberger (1983), Tucker (2011)). Instead, *Mathematica's* precision bounds are sometimes obtained using faster methods of the Jenkins-Traub variety (see Section I.1), which work correctly in theory but which are difficult to implement perfectly. Second, *Mathematica's* precision tracking is a black box: the specific algorithms it employs are proprietary.

We contend with these issues by restricting our use of *Mathematica's* numerical evaluation and precision tracking to a few clearly delineated cases: the evaluation of algebraic numbers, and the basic arithmetic operations of addition, subtraction, multiplication, and division. In particular, we do not use *Mathematica* for precision tracking in the computation of matrix inverses or the solution of linear systems, operations for which interval arithmetic does not generally provide clean answers (Alefeld and Herzberger (1983)). While one could insist that interval arithmetic be used for all non-exact calculations, we chose not to do so.

## II. The `BEP_Centipede.nb` notebook

In this section we describe the main functions from the `BEP_Centipede.nb` notebook, which contains all of the procedures we use to analyze BEP dynamics. Section II.1 describes functions used to prove analytical results, and Section II.2 describes the functions used in numerical analyses and in approximations with error bounds (cf. Proposition III.4). More details about the use of these functions are provided in the `BEP_Centipede.nb` notebook itself. Section II.3 explains the algorithms used to compute numerical values of rest points of the dynamics and eigenvalues of their derivative matrices.

Unless stated otherwise, the functions described below take a test-set rule  $\tau \in \{\tau^{\text{all}}, \tau^{\text{two}}, \tau^{\text{adj}}\}$ , a tie-breaking rule  $\beta \in \{\beta^{\text{min}}, \beta^{\text{stick}}, \beta^{\text{unif}}\}$  and a length  $d$  of the Centipede game as parameters. All functions besides the last two are for BEP dynamics with number of trials  $\kappa = 1$ . The `BEP_Centipede.nb` notebook includes examples of the use of each of the functions.

### II.1 Exact analysis

The functions for exact analysis of BEP dynamics in Centipede are as follows:

`ExactRestPoints` Uses `GroebnerBasis` and `Reduce` to compute the exact rest points of the dynamic.

`InstabilityOfVertexRestPoint` Conducts an analysis of the local stability of the vertex rest point  $\xi^\dagger$ . To do this, the function computes the derivative matrix  $D\mathcal{V}(\xi^\dagger)$  of the dynamic and the eigenvalues and eigenvectors of  $DV(\xi^\dagger)$ , where  $V: \text{aff}(\Xi) \rightarrow T\Xi$  (see Appendix A). Finally, the function reports whether one can conclude that  $\xi^\dagger$  is unstable. The function was not used explicitly in our analysis. Instead, we used it to determine the form of the derivative matrix, eigenvalues, and eigenvectors for arbitrary values of  $d$ ; see Appendix A and Section IV below.

`LocalStabilityOfInteriorRestPoint` Conducts an analysis of the local stability of the interior rest point  $\xi^*$ . To do this, the function computes a rational approximation  $\xi$  of the exact interior rest point  $\xi^*$ . The function then evaluates the eigenvalues of  $DV(\xi)$ , evaluates the perturbation bound from Proposition III.4 (which combines arguments from Appendix B and Section III), and reports whether one can conclude that  $\xi^*$  is asymptotically stable. See Section III for further details.

`GlobalStabilityOfInteriorRestPoint` Conducts an analysis of the global stability of the interior rest point  $\xi^*$ . To do this, the function uses `CylindricalDecomposition` to determine whether the relevant Lyapunov function (see Sections 5.2 and 6.1) is a strict Lyapunov function for the interior rest point  $\xi^*$  on domain  $\Xi \setminus \{\xi^\dagger\}$ . We did not use this function in our analysis because it fails to terminate under the settings for exact computation described in Section I.3.

## II.2 Numerical analysis

The following functions from the `BEP_Centipede.nb` are used for numerical analysis and as subroutines for `LocalStabilityOfInteriorRestPoint`.

`FloatingPointApproximateRestPoint` Computes a floating point approximation of the stable interior rest point of the BEP dynamic. See Section II.3 for details.

`RationalApproximateRestPoint` Computes a rational approximation of the stable interior rest point of the BEP dynamic. See Section II.3 for details.

`EigenvaluesAtRationalApproximateRestPoint` Computes the exact eigenvalues of  $DV(\xi)$ , where  $\xi$  is the rational approximation to the interior rest point obtained from a call to `RationalApproximateRestPoint`. See Section II.3 for details.

`NEigenvaluesAtRationalApproximateRestPoint` Computes the eigenvalues of  $DV(\tilde{\xi})$  using arbitrary-precision arithmetic, where  $\tilde{\xi}$  is a 16-digit precision approximation to the rational point computed using `RationalApproximateRestPoint`. See Section II.3 for details.

`NumericalGlobalStabilityOfInteriorRestPointLyapunov` Evaluates the time derivative  $\dot{\Lambda}(\xi) = \nabla\Lambda(\xi)'V(\xi)$  at a floating-point approximation  $\Lambda$  of the appropriate candidate Lyapunov function  $L$  for the interior rest point  $\xi^*$ , reporting instances in which the time derivative is not negative should any exist. The (presumably large number of) states  $\xi$  at which to evaluate  $\dot{\Lambda}(\xi)$  is chosen by the user.

`NumericalGlobalStabilityOfInteriorRestPointNDSolve` Computes numerical solutions to the BEP dynamic from initial conditions provided by the user, and reports whether any of these numerical solutions fails to converge to a neighborhood of the interior rest point  $\xi^*$ .

`NDSolveMeanDynamics` Uses *Mathematica's* `NDSolve` function to compute a numerical solution to the BEP dynamic from an initial condition provided by the user. The solution is computed until the time at which the norm of the law of motion is sufficiently small, where what constitutes sufficiently small can be chosen by the user. The function also graphs the components of the state as a function of time, and reports the terminal point and the time at which this point is reached.

`FloatingPointApproximateRestPointTestAllMinIfTieManyTrials` Uses *Mathematica's* `FindRoot` function to compute a floating point approximation of a rest point of the  $\text{BEP}(\tau^{\text{all}}, \kappa, \beta^{\text{min}})$  dynamic, where the number of trials  $\kappa$  is specified by the user. The function returns only one rest point. When there is more than one rest point, which one is computed depends strongly on the initial condition given to the function as an input. This function was used to produce Figures 4 and 5 and to compute the saddle points shown in Table 21.

`NDSolveMeanDynamicsTestAllMinIfTieManyTrials` Uses *Mathematica's* `NDSolve` function to compute a numerical solution of the  $\text{BEP}(\tau^{\text{all}}, \kappa, \beta^{\text{min}})$  dynamic, where the number of trials  $\kappa$  and the initial condition of the solution are specified by the user. The solution is computed until the time at which the norm of the law of motion is sufficiently small, where what constitutes sufficiently small can be chosen by the user. The function also graphs the components of the state as a function of time, and reports the terminal point and the time at which this point is reached. The function was used in producing Figure 6.

`EstimateSizeOfBasinOfAttractionOfVertexTestAllMinIfTieManyTrials` Provides an estimate of the size of the basin of attraction of the vertex rest point  $\xi^+$  under the  $\text{BEP}(\tau^{\text{all}}, \kappa, \beta^{\text{min}})$  dynamic. To do so, it discretizes the set of population states  $\Xi$  into a grid whose mesh is chosen by the user, and solves the dynamic with these grid points as initial conditions using *Mathematica's* `NDSolve` function. It returns the set of initial conditions from which the solution converges to  $\xi^+$ , and the set of all their neighbors in the grid. See Section VII for details.

### II.3 More on computation of approximate rest points and eigenvalues

The `BEP_Centipede.nb` notebook computes approximate rest points of  $\text{BEP}(\tau, 1, \beta)$  dynamics using the Euler method:  $\{\xi_t\}_{t=0}^T$  is computed starting from an initial condition  $\xi_0$  by iteratively applying

$$(1) \quad \xi_{t+1} = \xi_t + h \mathcal{V}(\xi_t),$$

where  $\mathcal{V}: \mathbb{R}^s \rightarrow \mathbb{R}^s$  is the (extended) law of motion of the dynamics and  $h$  is the step size of the algorithm. This algorithm is run in two sequential stages, to be described next.

When one of the first three `FloatingPointApproximateRestPoint...` functions from Section II.2 is called, algorithm (1) is run using IEEE 754 Standard double-precision floating-point arithmetic. The step size of the algorithm is set to  $h = 2^{-4}$ , and the initial condition is  $\xi_0 = (x_0, y_0) \in \Xi = (X, Y)$ , where  $x_0$  and  $y_0$  are the barycenters of simplices  $X$  and  $Y$ . Several thousand iterations of (1) are run, and the output of each iteration is projected onto  $\Xi$  to minimize the accumulation of roundoff errors from the floating-point calculation.

The floating-point numbers obtained in this way are very close to the exact quantities they approximate, but their digits (i.e., the values of the  $d_i$  in  $x = d_0.d_1d_2d_3d_4\dots \times 10^k$ ) may all be wrong, especially in small numbers, since many of the exact numbers we aim to approximate lie outside the range of IEEE 754 double-precision.<sup>3</sup>

To address this issue, the function `RationalApproximateRestPoint` begins with a call to `FloatingPointApproximateRestPoint`, and then uses the output of this procedure to create the initial condition for a second stage that employs rational arithmetic. This initial condition is the rational point in  $\Xi$  that lies closest to the floating-point output of the first stage. The step size  $h$  is set to 1 in the second stage, since overshooting is no longer a problem in the neighborhood of the exact rest point. Increment (1) is executed repeatedly using rational arithmetic until it locates a rational point  $\xi_T^*$  that is an approximate fixed point of (1), in the sense that  $\xi_T$  and  $\xi_{T+1} = \xi_T + \mathcal{V}(\xi_T)$  agree with 6 digits of precision for numbers greater or equal to  $10^{-4}$ , or 3 digits of precision for smaller numbers. This agrees with the format we use to report rest points in the tables in Section V.

`NEigenvaluesAtRationalApproximateRestPoint` computes the eigenvalues of  $DV(\tilde{\xi})$  using arbitrary-precision arithmetic, where  $\tilde{\xi}$  is a 16-digit precision approximation to the rational point computed by calling `RationalApproximateRestPoint`. The use of arbitrary precision allows us to keep track of the precision of the computed eigenvalues. Proposition III.4 provides a bound on the distances between the eigenvalues of  $DV(\tilde{\xi})$  and the eigenvalues of  $DV(\xi^*)$ . In the tables in Section VI, the reported eigenvalues, which are arbitrary-precision approximations to the (algebraic-valued) eigenvalues of  $DV(\xi)$ , are shown with 5 digits of precision for numbers greater or equal to 1, 4 digits of precision for numbers greater or equal to  $10^{-2}$ , and 3 digits of precision for smaller numbers.

### III. Dimension reduction for local stability analysis

This section presents the dimension reduction step used to reduce the computational demands of computing eigenvalue perturbation bounds, and presents a version of this bound (Proposition III.4) that incorporates all of the simplifications introduced here and in Appendix B.

Write  $a = s^1$ ,  $b = s^2$ , and  $s = s^1 + s^2$ , and recall that  $d = s - 2$ . The computations we use to prove local stability of the interior rest point require calculations involving the derivative matrices  $D\mathcal{V}(\xi) \in \mathbb{R}^{s \times s}$  that quickly become very computationally demanding

---

<sup>3</sup>For example, note that the IEEE 754 double-precision representation of numbers such as  $3.78 \times 10^{-681}$  and  $2.18 \times 10^{-20413}$  (both of which appear in Table 1 below) is 0, since both numbers are well below  $2^{-1074} \approx 4.94 \times 10^{-324}$ , which is the smallest positive IEEE 754 double-precision number.

as the size of the matrix grows. Since we are only interested in the action of  $D\mathcal{V}(\xi)$  on the  $d$ -dimensional subspace  $T\Xi$ , it should be possible to perform the desired calculations using matrices in  $\mathbb{R}^{d \times d}$ . We now show explicitly how this is done. The analysis is a simple extension of arguments from Sandholm (2007, p. 661).

Define the orthonormal matrix  $R \in \mathbb{R}^{s \times s}$  by

$$R = \left( \begin{array}{ccccc|ccccc} \frac{\sqrt{a-a}}{a(a-1)} + 1 & \frac{\sqrt{a-a}}{a(a-1)} & \cdots & \frac{\sqrt{a-a}}{a(a-1)} & -\frac{\sqrt{a}}{a} & 0 & \cdots & \cdots & \cdots & 0 \\ \frac{\sqrt{a-a}}{a(a-1)} & \frac{\sqrt{a-a}}{a(a-1)} + 1 & \ddots & \ddots & \vdots & \vdots & \ddots & \ddots & \ddots & \vdots \\ \frac{\sqrt{a-a}}{a(a-1)} & \ddots & \ddots & \frac{\sqrt{a-a}}{a(a-1)} & \vdots & \vdots & \ddots & \ddots & \ddots & \vdots \\ \frac{\sqrt{a-a}}{a(a-1)} & \cdots & \frac{\sqrt{a-a}}{a(a-1)} & \frac{\sqrt{a-a}}{a(a-1)} + 1 & -\frac{\sqrt{a}}{a} & \vdots & \ddots & \ddots & \ddots & \vdots \\ \frac{\sqrt{a}}{a} & \cdots & \cdots & \cdots & \frac{\sqrt{a}}{a} & 0 & \cdots & \cdots & \cdots & 0 \\ \hline 0 & \cdots & \cdots & \cdots & 0 & \frac{\sqrt{b-b}}{b(b-1)} + 1 & \frac{\sqrt{b-b}}{b(b-1)} & \cdots & \frac{\sqrt{b-b}}{b(b-1)} & -\frac{\sqrt{b}}{b} \\ \vdots & \ddots & \ddots & \ddots & \vdots & \frac{\sqrt{b-b}}{b(b-1)} & \frac{\sqrt{b-b}}{b(b-1)} + 1 & \ddots & \ddots & \vdots \\ \vdots & \ddots & \ddots & \ddots & \vdots & \frac{\sqrt{b-b}}{b(b-1)} & \ddots & \ddots & \frac{\sqrt{b-b}}{b(b-1)} & \vdots \\ \vdots & \ddots & \ddots & \ddots & \vdots & \frac{\sqrt{b-b}}{b(b-1)} & \cdots & \frac{\sqrt{b-b}}{b(b-1)} & \frac{\sqrt{b-b}}{b(b-1)} + 1 & -\frac{\sqrt{b}}{b} \\ 0 & \cdots & \cdots & \cdots & 0 & \frac{\sqrt{b}}{b} & \cdots & \cdots & \cdots & \frac{\sqrt{b}}{b} \end{array} \right).$$

Define the matrix  $J \in \mathbb{R}^{d \times s}$

$$J = \left( \begin{array}{ccccc|ccccc} 1 & 0 & \cdots & 0 & 0 & 0 & \cdots & \cdots & \cdots & 0 \\ 0 & \ddots & \ddots & \vdots & \vdots & \vdots & \ddots & \ddots & \ddots & \vdots \\ \vdots & \ddots & \ddots & 0 & \vdots & \vdots & \ddots & \ddots & \ddots & \vdots \\ 0 & \cdots & 0 & 1 & 0 & 0 & \cdots & \cdots & \cdots & 0 \\ \hline 0 & \cdots & \cdots & \cdots & 0 & 1 & 0 & \cdots & 0 & 0 \\ \vdots & \ddots & \ddots & \ddots & \vdots & 0 & \ddots & \ddots & \vdots & \vdots \\ \vdots & \ddots & \ddots & \ddots & \vdots & \vdots & \ddots & \ddots & 0 & \vdots \\ 0 & \cdots & \cdots & \cdots & 0 & 0 & \cdots & 0 & 1 & 0 \end{array} \right).$$

Define  $\bar{R} \in \mathbb{R}^{d \times s}$  by  $\bar{R} = JR$ . In words,  $\bar{R}$  is  $R$  with the last row in each block removed.

Let  $e_a$  denote the last standard basis vector in  $\mathbb{R}^a$ . The upper diagonal block of  $R$  rotates

$$\text{span}\{\mathbf{1}, e_a\} = \text{span}\left\{\frac{1}{\sqrt{a}}\mathbf{1}, \sqrt{\frac{a}{a-1}}\left(e_a - \frac{1}{a}\mathbf{1}\right)\right\} \subset \mathbb{R}^a$$

about its orthogonal complement by an angle of  $\cos^{-1}(\frac{1}{\sqrt{a}})$ . It is easy to verify that this block maps  $\mathbf{1}$  to  $\sqrt{a}e_a$ , and so, by virtue of being orthonormal, maps  $T\Xi^1$  isometrically to  $\mathbb{R}_+^a = \{x \in \mathbb{R}^a : x_a = 0\}$ . Likewise, the lower diagonal block of  $R$  maps  $\mathbf{1}$  to  $\sqrt{b}e_b$  and maps  $T\Xi^2$  isometrically to  $\mathbb{R}_+^b = \{y \in \mathbb{R}^b : y_b = 0\}$ . Altogether, premultiplying  $z \in \mathbb{R}^s$  by  $R$  double-rotates  $z$  so that its  $T\Xi$  component lies in  $\mathbb{R}_+^a \times \mathbb{R}_+^b$ . Then premultiplying the result



by  $J$  removes the now-superfluous final coordinates of each block.

Recall from Appendix A that the vector field  $V$  maps  $\text{aff}(\Xi)$  to  $T\Xi$ , so that  $DV(\xi)z \in T\Xi$  for all  $\xi \in \Xi$  and  $z \in T\Xi$ , and that the extension  $\mathcal{V}$  of  $V$  maps  $\mathbb{R}^s$  to itself, so that  $D\mathcal{V}(\xi)$  also maps  $\mathbb{R}^s$  to itself.

**Proposition III.1.** *If  $\xi \in \text{aff}(\Xi)$ , then  $DV(\xi)$  and  $\bar{R}D\mathcal{V}(\xi)\bar{R}'$  have the same eigenvalues, including multiplicities.*

Proposition III.1 is an immediate corollary of the following lemma:

**Lemma III.2.** *Suppose that  $M \in \mathbb{R}^{s \times s}$  maps  $T\Xi$  into itself, and let  $z \in \mathbb{C}^s$  be an element of the complexification of  $T\Xi$ . Then  $(\lambda, z)$  is an eigenvalue/eigenvector pair of  $M$  if and only if  $(\lambda, \bar{R}z)$  is an eigenvalue/eigenvector pair for  $\bar{R}M\bar{R}'$ .*

*Proof.* The proof follows Sandholm (2007). To start, recall from Appendix A that  $\Phi \in \mathbb{R}^{s \times s}$  is the orthogonal projection of  $\mathbb{R}^s$  onto  $T\Xi$ , and note the following geometrically obvious facts, each of which can be verified by direct computation:

$$(2) \quad \bar{R}'\bar{R} = R'J'JR = \Phi \in \mathbb{R}^{s \times s},$$

$$(3) \quad \bar{R}\bar{R}' = JRR'J' = JJ' = I \in \mathbb{R}^{d \times d}.$$

If  $Mz = \lambda z$ , then since  $Mz$  and  $z$  are in the complexification of  $T\Xi$ , we have  $\bar{R}M\Phi z = \lambda \bar{R}\Phi z$ ; thus (2) and (3) imply that  $\bar{R}M\bar{R}'\bar{R}z = \lambda \bar{R}\bar{R}'\bar{R}z = \lambda \bar{R}z$ . Conversely, if  $\bar{R}M\bar{R}'\bar{R}z = \lambda \bar{R}z$ , then (2) implies that  $\bar{R}M\Phi z = \bar{R}Mz = \lambda \bar{R}z$ , and so that  $Mz = \lambda z$ . ■

The following result is also needed to obtain the eigenvalue bound.

**Proposition III.3.** *For  $M, M^* \in \mathbb{R}^{s \times s}$ ,  $\|\bar{R}M\bar{R}' - \bar{R}M^*\bar{R}'\|_\infty \leq 4 \|M - M^*\|_\infty$ .*

*Proof.* Using the submultiplicativity of matrix norms and the orthonormality of  $R$ ,

$$\begin{aligned} \|\bar{R}M\bar{R}' - \bar{R}M^*\bar{R}'\|_\infty &\leq \|RMR' - RM^*R'\|_\infty \\ &= \|R(M - M^*)R'\|_\infty \\ &\leq \|R\|_\infty \|R'\|_\infty \|R'R(M - M^*)R'R\|_\infty \\ &\leq 4 \|M - M^*\|_\infty. \quad \blacksquare \end{aligned}$$

Using the results above and the arguments from Appendix B, including the definition

$$\Delta = \max_{i \in S} \max_{k \in S} \sum_{j \in S} \frac{\partial^2 \mathcal{V}'_i}{\partial \xi_j \partial \xi_k} (1, \dots, 1 | 1, \dots, 1),$$

we obtain the following result:

**Proposition III.4.** *Suppose that  $\bar{R}D\mathcal{V}(\xi)\bar{R}'$  is complex diagonalizable with  $\bar{R}D\mathcal{V}(\xi)\bar{R}' = \bar{Q} \text{diag}(\lambda)\bar{Q}^{-1}$ , and let  $\lambda^*$  be an eigenvalue of  $DV(\xi^*)$ . Then there is an eigenvalue  $\lambda_i$  of  $DV(\xi)$  such that*

$$(4) \quad |\lambda^* - \lambda_i| < \frac{8\Delta}{d^{d/2-1}} \frac{\text{tr}(\bar{Q}^* \bar{Q})^{d/2}}{|\det(\bar{Q})|} \sum_{k \in S} |\xi_k - \xi_k^*|.$$

When the function `InstabilityOfVertexRestPoint` from the `BEP_Centipede.nb` notebook is called, the eigenvectors in the matrix  $Q$  are chosen to have the Euclidean norm 1, as this tends to lower the bound on the condition number of  $Q$  (see Guggenheimer et al. (1995)). If this normalization were performed exactly, then we would have  $\text{tr}(\bar{Q}^* \bar{Q}) = d$ , allowing us to simplify inequality (4). However, because `InstabilityOfVertexRestPoint` performs the normalization after converting the entries of  $Q$  to arbitrary precision numbers, it uses the original inequality (4). Of course, the effect of this choice on the bound we obtain is essentially nil.

## IV. Repulsion from the backward induction state under test-adjacent

In games like *Centipede*, in which strategies are numbered according to when they end play, it is natural to consider test-set rules that account for the order relation on strategies. The simplest such rule, *test-adjacent* ( $\tau^{\text{adj}}$ ), has a revising agent tests his current strategy and an adjacent alternative, chosen at random when more than one is available. In this section, we prove:

**Proposition IV.1.** *In Centipede games of all lengths  $d$ , the backward induction state  $\xi^+$  is repelling under the  $\text{BEP}(\tau^{\text{adj}}, 1, \beta^{\text{min}})$  and  $\text{BEP}(\tau^{\text{adj}}, 1, \beta^{\text{stick}})$  dynamics.*

### IV.1 Test-adjacent, min-if-tie

Under the  $\text{BEP}(\tau^{\text{adj}}, 1, \beta^{\text{min}})$  dynamic,

$$D\mathcal{V}(\xi^+) = \left( \begin{array}{ccccc|ccccc} 0 & \frac{1}{2} & 0 & \cdots & 0 & 2 & 1 & \cdots & \cdots & 1 \\ 0 & -\frac{1}{2} & \ddots & \ddots & \vdots & 0 & 1 & \cdots & \cdots & 1 \\ \vdots & \ddots & \ddots & \frac{1}{2} & 0 & 0 & \cdots & \cdots & \cdots & 0 \\ \vdots & \ddots & \ddots & -\frac{1}{2} & 1 & \vdots & \ddots & \ddots & \ddots & \vdots \\ 0 & \cdots & \cdots & 0 & -1 & 0 & \cdots & \cdots & \cdots & 0 \\ \hline 2 & 1 & \cdots & \cdots & 1 & 0 & \frac{1}{2} & 0 & \cdots & 0 \\ 0 & 1 & \cdots & \cdots & 1 & 0 & -\frac{1}{2} & \ddots & \ddots & \vdots \\ 0 & \cdots & \cdots & \cdots & 0 & \vdots & \ddots & \ddots & \frac{1}{2} & 0 \\ \vdots & \ddots & \ddots & \ddots & \vdots & \vdots & \ddots & \ddots & -\frac{1}{2} & 1 \\ 0 & \cdots & \cdots & \cdots & 0 & 0 & \cdots & \cdots & 0 & -1 \end{array} \right)$$

We first consider the case in which  $d = 3$ , for which the eigenvalues and eigenvectors of  $DV(x^+, y^+)$  with respect to  $T\Xi$  are:

$$(5) \quad -1, \quad (0, 2, -2 \mid -1, 1)';$$

$$(6) \quad \lambda_- \equiv \frac{-3-\sqrt{17}}{4}, \quad (\lambda_- + 1, -\lambda_- - 1, 0 | 1, -1)'; \text{ and}$$

$$(7) \quad \lambda_+ \equiv \frac{-3+\sqrt{17}}{4}, \quad (\lambda_+ + 1, -\lambda_+ - 1, 0 | 1, -1)'.$$

The eigenvectors in (5) and (6) span the stable subspace  $E^s$  of the linear equation  $\dot{z} = DV(\xi^+)z$ . The normal vector to  $E^s$  is

$$z^\perp = \left(-\frac{2+\sqrt{17}}{3}, \frac{\sqrt{17}-1}{6}, \frac{5+\sqrt{17}}{6} \mid -1, 1\right)', \text{ which satisfies}$$

$$(z^\perp)'(\delta^2 - \delta^1) = \frac{1+\sqrt{17}}{2}, \quad (z^\perp)'(\delta^3 - \delta^1) = \frac{3+\sqrt{17}}{2}, \quad \text{and } (z^\perp)'(\varepsilon^2 - \varepsilon^1) = 2,$$

so the same arguments as above imply that  $\xi^+$  is a repeller.

For  $d \geq 4$ , the eigenvalues of  $DV(\xi^+)$  with respect to  $T\Xi$  are  $\frac{1}{2}$ ,  $-\frac{3}{2}$ ,  $-1$  (with algebraic multiplicity 2), and  $-\frac{1}{2}$  (with algebraic multiplicity  $d-4$ ). In the first three cases, the bases for the corresponding eigenspaces are as follows:

$$(8) \quad \frac{1}{2}, \quad \{\delta^2 - \delta^1 + \varepsilon^2 - \varepsilon^1\};$$

$$(9) \quad -\frac{3}{2}, \quad \{\delta^1 - \delta^2 + \varepsilon^2 - \varepsilon^1\};$$

$$(10) \quad -1, \quad \left\{ \delta^1 + 2 \sum_{i=3}^m (-1)^i \delta^i + (-1)^{m+1} \delta^{m+1} - \varepsilon^1 - 2 \sum_{j=3}^n (-1)^j \varepsilon^j - (-1)^{n+1} \varepsilon^{n+1}; \right. \\ \left. \frac{1}{2} \delta^1 + \delta^2 + 3 \sum_{i=3}^m (-1)^i \delta^i + \frac{3}{2} (-1)^{m+1} \delta^{m+1} - \varepsilon^1 + \varepsilon^2 \right\}.$$

The geometric multiplicity of the eigenvalue  $-\frac{1}{2}$  is 1 if  $d = 5$  and is 2 if  $d \geq 6$ . Thus for  $d \geq 7$ ,  $DV(\xi^+)$  is not diagonalizable. The generalized eigenvectors for the eigenvalue  $-\frac{1}{2}$ , which correspond to two blocks of the real Jordan matrix similar to  $DV(\xi^+)$ , are the  $m-2$  and  $n-2$  columns of the following two matrices:

$$(11) \quad \left( \begin{array}{cccccccc|cccc} 0 & 2 & -2 & 0 & 0 & 0 & \dots & 0 & -1 & 1 & 0 & \dots & 0 \\ -1 & 1 & 4 & -4 & 0 & 0 & \dots & 0 & 0 & 0 & 0 & \dots & 0 \\ 0 & -2 & 2 & 8 & -8 & 0 & \dots & 0 & 0 & 0 & 0 & \dots & 0 \\ \vdots & \ddots & \ddots & \ddots & \ddots & \ddots & \ddots & \vdots & \vdots & \vdots & \ddots & \vdots & \vdots \\ 0 & \dots & 0 & -2^{m-4} & 2^{m-4} & 2^{m-2} & -2^{m-2} & 0 & 0 & 0 & 0 & \dots & 0 \end{array} \right)' \text{ and}$$

$$(12) \quad \left( \begin{array}{cccccccc|cccccccc} \frac{1}{2} & \frac{3}{2} & -2 & 0 & 0 & 0 & 0 & \dots & 0 & -1 & 0 & 1 & 0 & 0 & 0 & 0 & \dots & 0 \\ 0 & 5 & -1 & -4 & 0 & 0 & 0 & \dots & 0 & -2 & 0 & 0 & 2 & 0 & 0 & 0 & \dots & 0 \\ 0 & 8 & 2 & -2 & -8 & 0 & 0 & \dots & \vdots & -4 & 0 & 0 & 0 & 4 & 0 & 0 & \dots & 0 \\ 0 & 16 & 0 & 4 & -4 & -16 & 0 & \dots & 0 & -8 & 0 & 0 & 0 & 0 & 8 & 0 & \dots & 0 \\ \vdots & \vdots & \vdots & \ddots & \ddots & \ddots & \ddots & \ddots & \vdots & \vdots & \vdots & \vdots & \vdots & \vdots & \ddots & \ddots & \ddots & \vdots \\ 0 & 2^{n-2} & 0 & \dots & 0 & 2^{n-4} & -2^{n-4} & -2^{n-2} & 0 & -2^{n-3} & 0 & 0 & 0 & 0 & \dots & 0 & 2^{n-3} & 0 \end{array} \right)'.$$

The eigenvectors in (10)–(12) span the stable subspace  $E^s$  of the linear equation  $\dot{z} = DV(\xi^+)z$ . The normal vector to  $E^s$  is the orthogonal projection onto  $T\Xi$  of the auxiliary vector

$$z_{\text{aux}}^\perp = \sum_{i=1}^m (2^{2-m} - 3 \cdot 2^{1-i}) \delta^i + \sum_{j=1}^n (2^{2-n} - 3 \cdot 2^{1-j}) \varepsilon^j.$$

Thus  $z^\perp$  satisfies

$$\begin{aligned} (z^\perp)'(\delta^{m+1} - \delta^1) &= (z_{\text{aux}}^\perp)'(\delta^{m+1} - \delta^1) = 3 - 2^{2-m} > 0, \\ (z^\perp)'(\varepsilon^{n+1} - \varepsilon^1) &= (z_{\text{aux}}^\perp)'(\varepsilon^{n+1} - \varepsilon^1) = 3 - 2^{2-n} > 0, \\ (z^\perp)'(\delta^i - \delta^1) &= (z_{\text{aux}}^\perp)'(\delta^i - \delta^1) = 3 \cdot (1 - 2^{1-i}) > 0 \text{ for } i \in S^1 \setminus \{1, m+1\}, \text{ and} \\ (z^\perp)'(\varepsilon^j - \varepsilon^1) &= (z_{\text{aux}}^\perp)'(\varepsilon^j - \varepsilon^1) = 3 \cdot (1 - 2^{1-j}) > 0 \text{ for } j \in S^2 \setminus \{1, n+1\}. \end{aligned}$$

Since the remaining eigenvalue, from (8), is positive, the arguments from the start of the section imply that  $\xi^\dagger$  is a repellor.

## IV.2 Test-adjacent, stick-if-tie:

Under the  $\text{BEP}(\tau^{\text{adj}}, 1, \beta^{\text{stick}})$  dynamic,

$$DV(x^\circ, y^\circ) = \left( \begin{array}{cccc|cccc} 0 & \frac{1}{2} & 0 & \dots & 0 & 2 & 1 & 1 & \dots & 1 \\ 0 & -\frac{1}{2} & 0 & \dots & 0 & 0 & 1 & 1 & \dots & 1 \\ 0 & 0 & 0 & \dots & 0 & 0 & 0 & 0 & \dots & 0 \\ \vdots & \vdots & \vdots & \dots & \vdots & \vdots & \vdots & \vdots & \dots & \vdots \\ 0 & 0 & 0 & \dots & 0 & 0 & 0 & 0 & \dots & 0 \\ \hline 2 & 1 & 1 & \dots & 1 & 0 & 0 & 0 & \dots & 0 \\ 0 & 1 & 1 & \dots & 1 & 0 & 0 & 0 & \dots & 0 \\ 0 & 0 & 0 & \dots & 0 & 0 & 0 & 0 & \dots & 0 \\ \vdots & \vdots & \vdots & \dots & \vdots & \vdots & \vdots & \vdots & \dots & \vdots \\ 0 & 0 & 0 & \dots & 0 & 0 & 0 & 0 & \dots & 0 \end{array} \right)$$

For  $d \geq 3$ , the eigenvalues of  $DV(\xi^\dagger)$  with respect to  $T\Xi$  and the bases for their eigenspaces are:

$$(13) \quad 0, \quad \left\{ 2(\delta^2 - \delta^3) - \varepsilon^1 + \varepsilon^2 \right\} \cup \left\{ \varepsilon^2 - \varepsilon^j : j \in \{3, \dots, s^2\} \right\} \text{ if } d \geq 4 \\ \cup \left\{ \delta^3 - \delta^i : i \in \{4, \dots, s^1\} \right\} \text{ if } d \geq 5;$$

$$(14) \quad \lambda_- \equiv -\frac{\sqrt{17}+1}{4}, \left\{ (-\lambda_-, \lambda_-, 0, \dots, 0 \mid -1, 1, 0, \dots, 0)' \right\}; \text{ and}$$

$$(15) \quad \lambda_+ \equiv \frac{\sqrt{17}-1}{4}, \left\{ (-\lambda_+, \lambda_+, 0, \dots, 0 \mid -1, 1, 0, \dots, 0)' \right\}.$$

The eigenvectors in (13) span the center subspace  $E^c$  of the linear equation  $\dot{z} = DV(\xi^\dagger)z$ , while the eigenvector in (14) spans the stable subspace  $E^s$ . The normal vector to the hyperplane  $E^c \oplus E^s$  is the orthogonal projection onto  $T\Xi$  of the auxiliary vector

$$z_{aux}^\perp = \left(\frac{1}{\lambda_-} - \frac{1}{2}\right)\delta^1 - \frac{1}{2}\delta^2 - \varepsilon^1$$

which satisfies

$$\begin{aligned} (z^\perp)'(\delta^2 - \delta^1) &= (z_{aux}^\perp)'(\delta^2 - \delta^1) = -\frac{1}{\lambda_-} > 0, \\ (z^\perp)'(\delta^i - \delta^1) &= (z_{aux}^\perp)'(\delta^i - \delta^1) = -\lambda_- > 0 \text{ for } i \in S^1 \setminus \{1, 2\}, \text{ and} \\ (z^\perp)'(\varepsilon^j - \varepsilon^1) &= (z_{aux}^\perp)'(\varepsilon^j - \delta^1) = 1 > 0 \text{ for } j \in S^2 \setminus \{1\}. \end{aligned}$$

Since the remaining eigenvalue, from (15), is positive, the arguments used in the appendix for  $\text{BEP}(\tau^{\text{all}}, 1, \beta^{\text{stick}})$  imply that  $\xi^\dagger$  is a repellor.

## V. Approximate components of attractor $\xi^*$ of $\text{BEP}(\tau, 1, \beta)$ dynamics

The tables in this section present approximate components of the unique interior rest points of  $\text{BEP}(\tau, 1, \beta)$  dynamics in Centipede games of lengths up to  $d = 20$ . Dashed lines in the tables separate cases in which the values were originally computed exactly from those in which the values were computed numerically.

Tables 1, 2, and 3 present the approximate rest points of the  $\text{BEP}(\tau^{\text{all}}, 1, \beta)$  dynamics with  $\beta = \beta^{\text{min}}, \beta^{\text{stick}},$  and  $\beta^{\text{unif}}$ . The approximate rest points of the  $\text{BEP}(\tau^{\text{two}}, 1, \beta)$  dynamics are presented in Tables 4–6, and those of the  $\text{BEP}(\tau^{\text{adj}}, 1, \beta)$  dynamics are presented in Tables 7–9.

The main text contains graphs of the rest points as a function of  $d$  for  $\text{BEP}(\tau^{\text{all}}, 1, \beta^{\text{min}})$  and  $\text{BEP}(\tau^{\text{two}}, 1, \beta^{\text{min}})$ . Graphs for the remaining seven cases appear here as Figures 1–7.

## V.1 Test-all

$p$	[6]	[5]	[4]	[3]	[2]	[1]	[0]
3	-	-	-	-	-	.618034	.381966
4	-	-	-	-	.113625	.501712	.384663
5	-	-	-	-	.113493	.501849	.384658
6	-	-	-	$3.12 \times 10^{-9}$	.113493	.501849	.384658
7	-	-	-	$3.12 \times 10^{-9}$	.113493	.501849	.384658
8	-	-	$8.23 \times 10^{-137}$	$3.12 \times 10^{-9}$	.113493	.501849	.384658
9	-	-	$8.23 \times 10^{-137}$	$3.12 \times 10^{-9}$	.113493	.501849	.384658
10	-	$7.75 \times 10^{-3403}$	$8.23 \times 10^{-137}$	$3.12 \times 10^{-9}$	.113493	.501849	.384658
11	-	$7.75 \times 10^{-3403}$	$8.23 \times 10^{-137}$	$3.12 \times 10^{-9}$	.113493	.501849	.384658
12	$1.06 \times 10^{-122476}$	$7.75 \times 10^{-3403}$	$8.23 \times 10^{-137}$	$3.12 \times 10^{-9}$	.113493	.501849	.384658
$\vdots$	$\vdots$	$\vdots$	$\vdots$	$\vdots$	$\vdots$	$\vdots$	$\vdots$
20	$1.06 \times 10^{-122476}$	$7.75 \times 10^{-3403}$	$8.23 \times 10^{-137}$	$3.12 \times 10^{-9}$	.113493	.501849	.384658

$q$	[6]	[5]	[4]	[3]	[2]	[1]	[0]
3	-	-	-	-	.381966	.381966	.236068
4	-	-	-	-	.337084	.419741	.243175
5	-	-	-	.001462	.335672	.419706	.243160
6	-	-	-	.001462	.335672	.419706	.243160
7	-	-	$9.53 \times 10^{-35}$	.001462	.335672	.419706	.243160
8	-	-	$9.53 \times 10^{-35}$	.001462	.335672	.419706	.243160
9	-	$3.78 \times 10^{-681}$	$9.53 \times 10^{-35}$	.001462	.335672	.419706	.243160
10	-	$3.78 \times 10^{-681}$	$9.53 \times 10^{-35}$	.001462	.335672	.419706	.243160
11	$2.18 \times 10^{-20413}$	$3.78 \times 10^{-681}$	$9.53 \times 10^{-35}$	.001462	.335672	.419706	.243160
12	$2.18 \times 10^{-20413}$	$3.78 \times 10^{-681}$	$9.53 \times 10^{-35}$	.001462	.335672	.419706	.243160
$\vdots$	$\vdots$	$\vdots$	$\vdots$	$\vdots$	$\vdots$	$\vdots$	$\vdots$
20	$2.18 \times 10^{-20413}$	$3.78 \times 10^{-681}$	$9.53 \times 10^{-35}$	.001462	.335672	.419706	.243160

Table 1: The interior rest point of the  $\text{BEP}(\tau^{\text{all}}, 1, \beta^{\text{min}})$  dynamic for Centipede of lengths  $d \in \{3, \dots, 20\}$ .  $p$  denotes the penultimate player,  $q$  the last player. The dashed lines separated exact ( $d \leq 6$ ) from numerical ( $d \geq 7$ ) results.

$p$	[6]	[5]	[4]	[3]	[2]	[1]	[0]
2	-	-	-	-	-	.618034	.381966
3	-	-	-	-	-	.569840	.430160
4	-	-	-	-	.110240	.500220	.389541
5	-	-	-	-	.110647	.499886	.389467
6	-	-	-	$2.49 \times 10^{-9}$	.110647	.499886	.389467
7	-	-	-	$2.49 \times 10^{-9}$	.110647	.499886	.389467
8	-	-	$2.12 \times 10^{-138}$	$2.49 \times 10^{-9}$	.110647	.499886	.389467
9	-	-	$2.12 \times 10^{-138}$	$2.49 \times 10^{-9}$	.110647	.499886	.389467
10	-	$1.51 \times 10^{-3442}$	$2.12 \times 10^{-138}$	$2.49 \times 10^{-9}$	.110647	.499886	.389467
11	-	$1.51 \times 10^{-3442}$	$2.12 \times 10^{-138}$	$2.49 \times 10^{-9}$	.110647	.499886	.389467
12	$2.91 \times 10^{-123906}$	$1.51 \times 10^{-3442}$	$2.12 \times 10^{-138}$	$2.49 \times 10^{-9}$	.110647	.499886	.389467
$\vdots$	$\vdots$	$\vdots$	$\vdots$	$\vdots$	$\vdots$	$\vdots$	$\vdots$
20	$2.91 \times 10^{-123906}$	$1.51 \times 10^{-3442}$	$2.12 \times 10^{-138}$	$2.49 \times 10^{-9}$	.110647	.499886	.389467

$q$	[6]	[5]	[4]	[3]	[2]	[1]	[0]
2	-	-	-	-	-	.618034	.381966
3	-	-	-	-	.324718	.430160	.245122
4	-	-	-	-	.332023	.416835	.251142
5	-	-	-	.001355	.331507	.416301	.250838
6	-	-	-	.001355	.331507	.416301	.250838
7	-	-	$3.82 \times 10^{-35}$	.001355	.331507	.416301	.250838
8	-	-	$3.82 \times 10^{-35}$	.001355	.331507	.416301	.250838
9	-	$4.32 \times 10^{-689}$	$3.82 \times 10^{-35}$	.001355	.331507	.416301	.250838
10	-	$4.32 \times 10^{-689}$	$3.82 \times 10^{-35}$	.001355	.331507	.416301	.250838
11	$1.19 \times 10^{-20651}$	$4.32 \times 10^{-689}$	$3.82 \times 10^{-35}$	.001355	.331507	.416301	.250838
12	$1.19 \times 10^{-20651}$	$4.32 \times 10^{-689}$	$3.82 \times 10^{-35}$	.001355	.331507	.416301	.250838
$\vdots$	$\vdots$	$\vdots$	$\vdots$	$\vdots$	$\vdots$	$\vdots$	$\vdots$
20	$1.19 \times 10^{-20651}$	$4.32 \times 10^{-689}$	$3.82 \times 10^{-35}$	.001355	.331507	.416301	.250838

Table 2: The interior rest point of the  $\text{BEP}(\tau^{\text{all}}, 1, \beta^{\text{stick}})$  dynamic for Centipede of lengths  $d \in \{2, \dots, 20\}$ .  $p$  denotes the penultimate player,  $q$  the last player. The dashed lines separated exact ( $d \leq 5$ ) from numerical ( $d \geq 6$ ) results.

$p$	[6]	[5]	[4]	[3]	[2]	[1]	[0]
2	-	-	-	-	-	.585786	.414214
3	-	-	-	-	-	.564579	.435421
4	-	-	-	-	.107649	.498332	.394019
5	-	-	-	-	.108048	.498041	.393911
6	-	-	-	$2.01 \times 10^{-9}$	.108048	.498041	.393911
7	-	-	-	$2.01 \times 10^{-9}$	.108048	.498041	.393911
8	-	-	$6.93 \times 10^{-140}$	$2.01 \times 10^{-9}$	.108048	.498041	.393911
9	-	-	$6.93 \times 10^{-140}$	$2.01 \times 10^{-9}$	.108048	.498041	.393911
10	-	$1.05 \times 10^{-3479}$	$6.93 \times 10^{-140}$	$2.01 \times 10^{-9}$	.108048	.498041	.393911
11	-	$1.05 \times 10^{-3479}$	$6.93 \times 10^{-140}$	$2.01 \times 10^{-9}$	.108048	.498041	.393911
12	$6.65 \times 10^{-125244}$	$1.05 \times 10^{-3479}$	$6.93 \times 10^{-140}$	$2.01 \times 10^{-9}$	.108048	.498041	.393911
$\vdots$	$\vdots$	$\vdots$	$\vdots$	$\vdots$	$\vdots$	$\vdots$	$\vdots$
20	$6.65 \times 10^{-125244}$	$1.05 \times 10^{-3479}$	$6.93 \times 10^{-140}$	$2.01 \times 10^{-9}$	.108048	.498041	.393911

$q$	[6]	[5]	[4]	[3]	[2]	[1]	[0]
2	-	-	-	-	-	.585786	.414214
3	-	-	-	-	.318750	.435421	.245829
4	-	-	-	-	.328099	.413576	.258325
5	-	-	-	.001261	.327653	.413126	.257960
6	-	-	-	.001261	.327653	.413126	.257960
7	-	-	$1.62 \times 10^{-35}$	.001261	.327653	.413126	.257960
8	-	-	$1.62 \times 10^{-35}$	.001261	.327653	.413126	.257960
9	-	$1.60 \times 10^{-696}$	$1.62 \times 10^{-35}$	.001261	.327653	.413126	.257960
10	-	$1.60 \times 10^{-696}$	$1.62 \times 10^{-35}$	.001261	.327653	.413126	.257960
11	$1.37 \times 10^{-20874}$	$1.60 \times 10^{-696}$	$1.62 \times 10^{-35}$	.001261	.327653	.413126	.257960
12	$1.37 \times 10^{-20874}$	$1.60 \times 10^{-696}$	$1.62 \times 10^{-35}$	.001261	.327653	.413126	.257960
$\vdots$	$\vdots$	$\vdots$	$\vdots$	$\vdots$	$\vdots$	$\vdots$	$\vdots$
20	$1.37 \times 10^{-20874}$	$1.60 \times 10^{-696}$	$1.62 \times 10^{-35}$	.001261	.327653	.413126	.257960

Table 3: The interior rest point of the  $\text{BEP}(\tau^{\text{all}}, 1, \beta^{\text{unif}})$  dynamic for Centipede of lengths  $d \in \{2, \dots, 20\}$ .  $p$  denotes the penultimate player,  $q$  the last player. The dashed lines separated exact ( $d \leq 6$ ) from numerical ( $d \geq 7$ ) results.



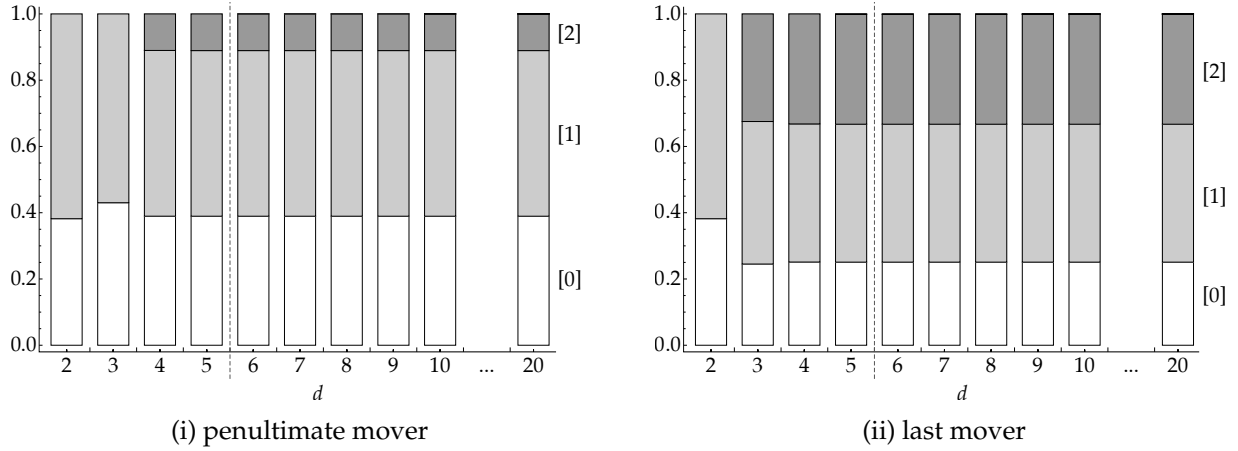


Figure 1: The stable rest point of Centipede under the  $\text{BEP}(\tau^{\text{all}}, 1, \beta^{\text{stick}})$  dynamic for game lengths  $d = 3, \dots, 10$  and  $d = 20$ . Stacked bars, from the bottom to the top, represent weights on strategy [0] (continue at all decision nodes), [1] (stop at the last node), [2] (stop at the second-to-last node), etc. The dashed line separates exact ( $d \leq 5$ ) and numerical ( $d \geq 6$ ) results.

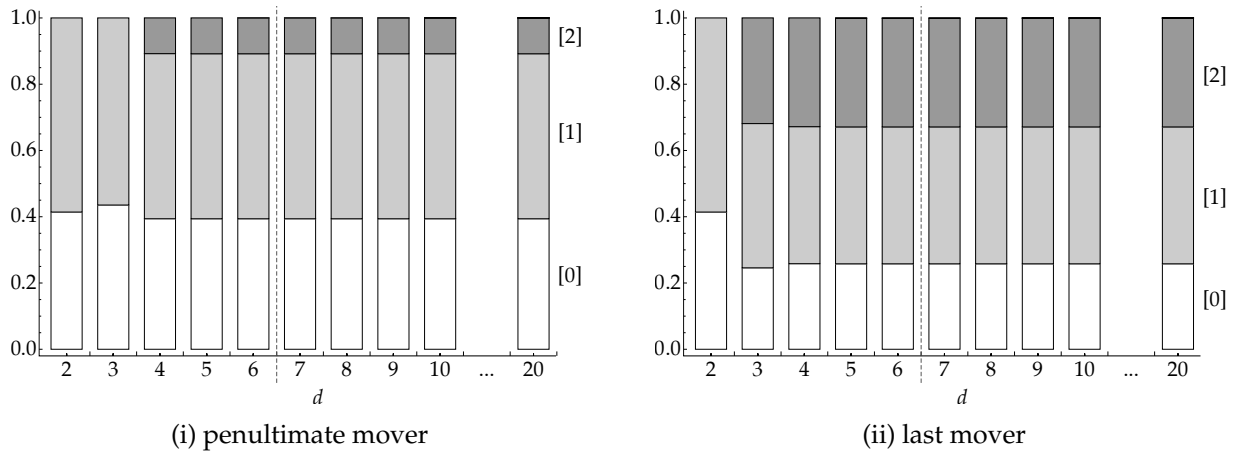


Figure 2: The stable rest point of Centipede under the  $\text{BEP}(\tau^{\text{all}}, 1, \beta^{\text{unif}})$  dynamic for game lengths  $d = 3, \dots, 10$  and  $d = 20$ . Stacked bars, from the bottom to the top, represent weights on strategies [0], [1], [2], etc. The dashed line separates exact ( $d \leq 6$ ) and numerical ( $d \geq 7$ ) results.

## V.2 Test-two

$p$	[7]	[6]	[5]	[4]	[3]	[2]	[1]	[0]
3	-	-	-	-	-	-	.666667	.333333
4	-	-	-	-	-	.257462	.435788	.306750
5	-	-	-	-	-	.263525	.417165	.319310
6	-	-	-	-	.042829	.255195	.391735	.310241
7	-	-	-	-	.048513	.255401	.386242	.309844
8	-	-	-	.003549	.050550	.254601	.382766	.308534
9	-	-	-	.003854	.051203	.254560	.382016	.308368
10	-	-	.000165	.003938	.051375	.254507	.381745	.308270
11	-	-	.000173	.003957	.051415	.254502	.381696	.308257
12	-	$4.98 \times 10^{-6}$	.000174	.003961	.051423	.254500	.381684	.308253
13	-	$5.14 \times 10^{-6}$	.000175	.003962	.051425	.254500	.381682	.308253
14	$1.08 \times 10^{-7}$	$5.17 \times 10^{-6}$	.000175	.003962	.051425	.254500	.381681	.308253
15	$1.10 \times 10^{-7}$	$5.17 \times 10^{-6}$	.000175	.003962	.051425	.254500	.381681	.308252
$\vdots$	$\vdots$	$\vdots$	$\vdots$	$\vdots$	$\vdots$	$\vdots$	$\vdots$	$\vdots$
20	$1.10 \times 10^{-7}$	$5.17 \times 10^{-6}$	.000175	.003962	.051425	.254500	.381681	.308252

$q$	[7]	[6]	[5]	[4]	[3]	[2]	[1]	[0]
3	-	-	-	-	-	.500000	.333333	.166667
4	-	-	-	-	-	.409494	.360668	.229837
5	-	-	-	-	.106563	.347606	.324311	.221520
6	-	-	-	-	.118350	.336191	.319434	.226026
7	-	-	-	.012586	.121612	.327768	.313291	.224742
8	-	-	-	.014048	.123313	.325699	.311961	.224979
9	-	-	.000773	.014479	.123730	.324832	.311317	.224870
10	-	-	.000823	.014600	.123865	.324645	.311189	.224877
11	-	$2.88 \times 10^{-5}$	.000834	.014627	.123892	.324595	.311152	.224872
12	-	$2.99 \times 10^{-5}$	.000837	.014633	.123898	.324585	.311145	.224872
13	$7.34 \times 10^{-7}$	$3.01 \times 10^{-5}$	.000837	.014634	.123899	.324584	.311144	.224872
14	$7.53 \times 10^{-7}$	$3.01 \times 10^{-5}$	.000837	.014634	.123899	.324583	.311144	.224872
15	$7.56 \times 10^{-7}$	$3.01 \times 10^{-5}$	.000837	.014634	.123899	.324583	.311144	.224872
16	$7.57 \times 10^{-7}$	$3.01 \times 10^{-5}$	.000837	.014634	.123899	.324583	.311144	.224872
$\vdots$	$\vdots$	$\vdots$	$\vdots$	$\vdots$	$\vdots$	$\vdots$	$\vdots$	$\vdots$
20	$7.57 \times 10^{-7}$	$3.01 \times 10^{-5}$	.000837	.014634	.123899	.324583	.311144	.224872

Table 4: The interior rest point of the  $\text{BEP}(\tau^{\text{two}}, 1, \beta^{\min})$  dynamic for Centipede of lengths  $d \in \{3, \dots, 20\}$ .  $p$  denotes the penultimate player,  $q$  the last player. The dashed lines separated exact ( $d \leq 8$ ) from numerical ( $d \geq 9$ ) results.

$p$	[7]	[6]	[5]	[4]	[3]	[2]	[1]	[0]
2	-	-	-	-	-	-	.618034	.381966
3	-	-	-	-	-	-	.539189	.460811
4	-	-	-	-	-	.208426	.411450	.380124
5	-	-	-	-	-	.223867	.398692	.377441
6	-	-	-	-	.035722	.223253	.378763	.362262
7	-	-	-	-	.040882	.225279	.374384	.359455
8	-	-	-	.002980	.042792	.225384	.371574	.357271
9	-	-	-	.003239	.043396	.225559	.370966	.356839
10	-	-	.000138	.003311	.043558	.225576	.370747	.356670
11	-	-	.000145	.003327	.043595	.225585	.370707	.356641
12	-	$4.19 \times 10^{-6}$	.000147	.003330	.043603	.225586	.370697	.356633
13	-	$4.32 \times 10^{-6}$	.000147	.003331	.043604	.225586	.370695	.356632
14	$9.04 \times 10^{-8}$	$4.34 \times 10^{-6}$	.000147	.003331	.043604	.225586	.370695	.356632
15	$9.24 \times 10^{-8}$	$4.34 \times 10^{-6}$	.000147	.003331	.043604	.225586	.370695	.356632
16	$9.27 \times 10^{-8}$	$4.34 \times 10^{-6}$	.000147	.003331	.043604	.225586	.370695	.356632
17	$9.28 \times 10^{-8}$	$4.34 \times 10^{-6}$	.000147	.003331	.043604	.225586	.370695	.356632
$\vdots$	$\vdots$	$\vdots$	$\vdots$	$\vdots$	$\vdots$	$\vdots$	$\vdots$	$\vdots$
20	$9.28 \times 10^{-8}$	$4.34 \times 10^{-6}$	.000147	.003331	.043604	.225586	.370695	.356632

$q$	[7]	[6]	[5]	[4]	[3]	[2]	[1]	[0]
2	-	-	-	-	-	-	.618034	.381966
3	-	-	-	-	-	.369102	.369102	.261795
4	-	-	-	-	-	.344955	.364555	.290490
5	-	-	-	-	.087713	.310211	.329668	.272409
6	-	-	-	-	.100021	.304394	.323241	.272345
7	-	-	-	.010544	.104027	.298920	.317193	.269316
8	-	-	-	.011813	.105888	.297664	.315745	.268891
9	-	-	.000650	.012191	.106378	.297094	.315103	.268585
10	-	-	.000692	.012297	.106528	.296977	.314969	.268537
11	-	$2.42 \times 10^{-5}$	.000701	.012321	.106559	.296944	.314931	.268520
12	-	$2.51 \times 10^{-5}$	.000703	.012326	.106566	.296938	.314925	.268518
13	$6.17 \times 10^{-7}$	$2.53 \times 10^{-5}$	.000703	.012327	.106567	.296937	.314923	.268517
14	$6.33 \times 10^{-7}$	$2.53 \times 10^{-5}$	.000703	.012327	.106567	.296936	.314923	.268517
15	$6.35 \times 10^{-7}$	$2.53 \times 10^{-5}$	.000703	.012327	.106567	.296936	.314923	.268517
16	$6.36 \times 10^{-7}$	$2.53 \times 10^{-5}$	.000703	.012327	.106567	.296936	.314923	.268517
$\vdots$	$\vdots$	$\vdots$	$\vdots$	$\vdots$	$\vdots$	$\vdots$	$\vdots$	$\vdots$
20	$6.36 \times 10^{-7}$	$2.53 \times 10^{-5}$	.000703	.012327	.106567	.296936	.314923	.268517

Table 5: The interior rest point of the  $\text{BEP}(\tau^{\text{two}}, 1, \beta^{\text{stick}})$  dynamic for Centipede of lengths  $d \in \{2, \dots, 20\}$ .  $p$  denotes the penultimate player,  $q$  the last player. The dashed lines separated exact ( $d \leq 8$ ) from numerical ( $d \geq 9$ ) results.

$p$	[7]	[6]	[5]	[4]	[3]	[2]	[1]	[0]
2	-	-	-	-	-	-	.585786	.414214
3	-	-	-	-	-	-	.529609	.470391
4	-	-	-	-	-	.206430	.409294	.384276
5	-	-	-	-	-	.223682	.396778	.379541
6	-	-	-	-	.035854	.223566	.377039	.363541
7	-	-	-	-	.041111	.225761	.372690	.360438
8	-	-	-	.002999	.043058	.225921	.369887	.358136
9	-	-	-	.003261	.043675	.226112	.369281	.357671
10	-	-	.000139	.003334	.043839	.226133	.369062	.357492
11	-	-	.000146	.003350	.043877	.226144	.369022	.357461
12	-	$4.22 \times 10^{-6}$	.000148	.003353	.043885	.226145	.369012	.357453
13	-	$4.35 \times 10^{-6}$	.000148	.003354	.043887	.226145	.369011	.357451
14	$9.11 \times 10^{-8}$	$4.37 \times 10^{-6}$	.000148	.003354	.043887	.226145	.369011	.357451
15	$9.31 \times 10^{-8}$	$4.37 \times 10^{-6}$	.000148	.003354	.043887	.226145	.369010	.357451
16	$9.34 \times 10^{-8}$	$4.37 \times 10^{-6}$	.000148	.003354	.043887	.226145	.369010	.357451
17	$9.34 \times 10^{-8}$	$4.38 \times 10^{-6}$	.000148	.003354	.043887	.226145	.369010	.357451
$\vdots$	$\vdots$	$\vdots$	$\vdots$	$\vdots$	$\vdots$	$\vdots$	$\vdots$	$\vdots$
20	$9.34 \times 10^{-8}$	$4.38 \times 10^{-6}$	.000148	.003354	.043887	.226145	.369010	.357451

$q$	[7]	[6]	[5]	[4]	[3]	[2]	[1]	[0]
2	-	-	-	-	-	-	.585786	.414214
3	-	-	-	-	-	.360182	.366186	.273632
4	-	-	-	-	-	.342216	.361057	.296727
5	-	-	-	-	.087628	.308865	.326875	.276633
6	-	-	-	-	.100366	.303312	.320604	.275717
7	-	-	-	.010605	.104522	.297912	.314635	.272326
8	-	-	-	.011890	.106443	.296679	.313212	.271775
9	-	-	.000654	.012273	.106951	.296114	.312579	.271429
10	-	-	.000696	.012381	.107106	.295999	.312446	.271371
11	-	$2.44 \times 10^{-5}$	.000706	.012405	.107138	.295966	.312409	.271351
12	-	$2.53 \times 10^{-5}$	.000708	.012410	.107146	.295961	.312403	.271348
13	$6.21 \times 10^{-7}$	$2.55 \times 10^{-5}$	.000708	.012411	.107147	.295959	.312401	.271347
14	$6.37 \times 10^{-7}$	$2.55 \times 10^{-5}$	.000708	.012411	.107147	.295959	.312401	.271347
15	$6.40 \times 10^{-7}$	$2.55 \times 10^{-5}$	.000708	.012411	.107147	.295959	.312401	.271347
$\vdots$	$\vdots$	$\vdots$	$\vdots$	$\vdots$	$\vdots$	$\vdots$	$\vdots$	$\vdots$
20	$6.40 \times 10^{-7}$	$2.55 \times 10^{-5}$	.000708	.012411	.107147	.295959	.312401	.271347

Table 6: The interior rest point of the  $\text{BEP}(\tau^{\text{two}}, 1, \beta^{\text{unif}})$  dynamic for Centipede of lengths  $d \in \{2, \dots, 20\}$ .  $p$  denotes the penultimate player,  $q$  the last player. The dashed lines separated exact ( $d \leq 8$ ) from numerical ( $d \geq 9$ ) results.

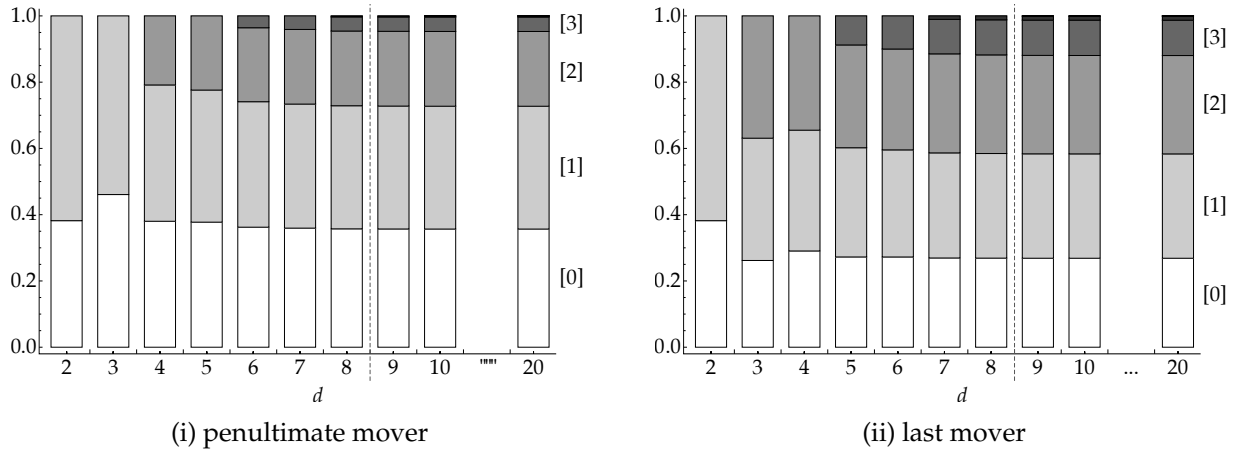


Figure 3: The stable rest point of Centipede under the  $\text{BEP}(\tau^{\text{two}}, 1, \beta^{\text{stick}})$  dynamic for game lengths  $d = 3, \dots, 10$  and  $d = 20$ . Stacked bars, from the bottom to the top, represent weights on strategies [0], [1], [2], etc. The dashed line separates exact ( $d \leq 8$ ) and numerical ( $d \geq 9$ ) results.

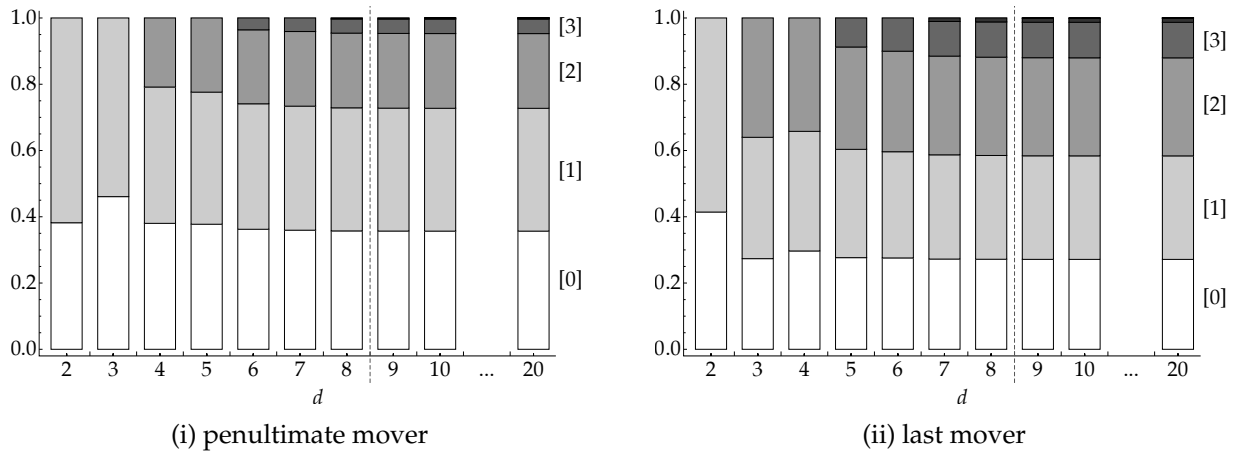


Figure 4: The stable rest point of Centipede under the  $\text{BEP}(\tau^{\text{two}}, 1, \beta^{\text{unif}})$  dynamic for game lengths  $d = 3, \dots, 10$  and  $d = 20$ . Stacked bars, from the bottom to the top, represent weights on strategies [0], [1], [2], etc. The dashed line separates exact ( $d \leq 8$ ) and numerical ( $d \geq 9$ ) results.

### V.3 Test-adjacent

$p$	[7]	[6]	[5]	[4]	[3]	[2]	[1]	[0]
3	-	-	-	-	-	-	.729473	.270527
4	-	-	-	-	-	.296372	.584389	.119239
5	-	-	-	-	-	.397177	.490705	.112118
6	-	-	-	-	.095463	.499705	.323347	.081485
7	-	-	-	-	.181047	.459731	.284081	.075141
8	-	-	-	.014840	.301960	.371559	.243321	.068320
9	-	-	-	.030316	.300216	.353575	.243038	.072854
10	-	-	.000144	.057357	.283552	.344163	.241557	.073227
11	-	-	.000296	.058116	.282139	.343333	.242261	.073856
12	-	$8.90 \times 10^{-10}$	.000593	.058071	.281958	.343249	.242262	.073866
13	-	$1.78 \times 10^{-9}$	.000593	.058072	.281957	.343249	.242263	.073867
14	$1.90 \times 10^{-23}$	$3.56 \times 10^{-9}$	.000593	.058072	.281957	.343249	.242263	.073867
15	$3.81 \times 10^{-23}$	$3.56 \times 10^{-9}$	.000593	.058072	.281957	.343249	.242263	.073867
16	$7.61 \times 10^{-23}$	$3.56 \times 10^{-9}$	.000593	.058072	.281957	.343249	.242263	.073867
$\vdots$	$\vdots$	$\vdots$	$\vdots$	$\vdots$	$\vdots$	$\vdots$	$\vdots$	$\vdots$
20	$7.61 \times 10^{-23}$	$3.56 \times 10^{-9}$	.000593	.058072	.281957	.343249	.242263	.073867

$q$	[7]	[6]	[5]	[4]	[3]	[2]	[1]	[0]
3	-	-	-	-	-	.545589	.404665	.049746
4	-	-	-	-	-	.503549	.416231	.080220
5	-	-	-	-	.176647	.536220	.237563	.049570
6	-	-	-	-	.276453	.457032	.216693	.049822
7	-	-	-	.045738	.413785	.328370	.169467	.042639
8	-	-	-	.089495	.394108	.301989	.168401	.046007
9	-	-	.002593	.165863	.350152	.277205	.159399	.044788
10	-	-	.005004	.164064	.341152	.277408	.164632	.047740
11	-	$1.49 \times 10^{-6}$	.010069	.162366	.338681	.276584	.164506	.047791
12	-	$3.00 \times 10^{-6}$	.010109	.162312	.338579	.276597	.164572	.047827
13	$5.34 \times 10^{-15}$	$6.00 \times 10^{-6}$	.010109	.162311	.338578	.276597	.164572	.047827
14	$1.07 \times 10^{-14}$	$6.00 \times 10^{-6}$	.010109	.162311	.338578	.276597	.164572	.047827
15	$2.14 \times 10^{-14}$	$6.00 \times 10^{-6}$	.010109	.162311	.338578	.276597	.164572	.047827
$\vdots$	$\vdots$	$\vdots$	$\vdots$	$\vdots$	$\vdots$	$\vdots$	$\vdots$	$\vdots$
20	$2.14 \times 10^{-14}$	$6.00 \times 10^{-6}$	.010109	.162311	.338578	.276597	.164572	.047827

Table 7: The interior rest point of the  $\text{BEP}(\tau^{\text{adj}}, 1, \beta^{\min})$  dynamic for Centipede of lengths  $d \in \{3, \dots, 20\}$ .  $p$  denotes the penultimate player,  $q$  the last player. The dashed lines separated exact ( $d \leq 7$ ) from numerical ( $d \geq 8$ ) results.

$p$	[7]	[6]	[5]	[4]	[3]	[2]	[1]	[0]
2	-	-	-	-	-	-	.618034	.381966
3	-	-	-	-	-	-	.618034	.381966
4	-	-	-	-	-	.199035	.590835	.210130
5	-	-	-	-	-	.279691	.509434	.210875
6	-	-	-	-	.033018	.390517	.406372	.170093
7	-	-	-	-	.063584	.373078	.392320	.171018
8	-	-	-	.001052	.120895	.345367	.370869	.161817
9	-	-	-	.002302	.125457	.342720	.368046	.161475
10	-	-	$1.98 \times 10^{-7}$	.004684	.125303	.341681	.367204	.161127
11	-	-	$3.99 \times 10^{-7}$	.004697	.125326	.341665	.367187	.161124
12	-	$2.70 \times 10^{-17}$	$7.98 \times 10^{-7}$	.004697	.125326	.341665	.367187	.161124
13	-	$5.40 \times 10^{-17}$	$7.98 \times 10^{-7}$	.004697	.125326	.341665	.367187	.161124
14	$3.95 \times 10^{-43}$	$1.08 \times 10^{-16}$	$7.98 \times 10^{-7}$	.004697	.125326	.341665	.367187	.161124
15	$7.90 \times 10^{-43}$	$1.08 \times 10^{-16}$	$7.98 \times 10^{-7}$	.004697	.125326	.341665	.367187	.161124
16	$1.58 \times 10^{-42}$	$1.08 \times 10^{-16}$	$7.98 \times 10^{-7}$	.004697	.125326	.341665	.367187	.161124
$\vdots$	$\vdots$	$\vdots$	$\vdots$	$\vdots$	$\vdots$	$\vdots$	$\vdots$	$\vdots$
20	$1.58 \times 10^{-42}$	$1.08 \times 10^{-16}$	$7.98 \times 10^{-7}$	.004697	.125326	.341665	.367187	.161124

$q$	[7]	[6]	[5]	[4]	[3]	[2]	[1]	[0]
2	-	-	-	-	-	-	.618034	.381966
3	-	-	-	-	-	.381966	.472136	.145898
4	-	-	-	-	-	.402536	.417039	.180426
5	-	-	-	-	.093004	.479038	.297798	.130161
6	-	-	-	-	.144642	.416292	.300882	.138184
7	-	-	-	.008418	.247934	.355962	.265529	.122157
8	-	-	-	.017105	.246616	.345439	.266729	.124111
9	-	-	$4.08 \times 10^{-5}$	.035361	.242053	.338091	.262323	.122131
10	-	-	$8.46 \times 10^{-5}$	.035956	.241953	.337562	.262280	.122165
11	-	$3.38 \times 10^{-11}$	.000170	.035964	.241930	.337524	.262258	.122155
12	-	$6.77 \times 10^{-11}$	.000170	.035964	.241930	.337524	.262258	.122155
13	$3.66 \times 10^{-27}$	$1.35 \times 10^{-10}$	.000170	.035964	.241930	.337524	.262258	.122155
14	$7.31 \times 10^{-27}$	$1.35 \times 10^{-10}$	.000170	.035964	.241930	.337524	.262258	.122155
15	$1.46 \times 10^{-26}$	$1.35 \times 10^{-10}$	.000170	.035964	.241930	.337524	.262258	.122155
$\vdots$	$\vdots$	$\vdots$	$\vdots$	$\vdots$	$\vdots$	$\vdots$	$\vdots$	$\vdots$
20	$1.46 \times 10^{-26}$	$1.35 \times 10^{-10}$	.000170	.035964	.241930	.337524	.262258	.122155

Table 8: The interior rest point of the  $\text{BEP}(\tau^{\text{adj}}, 1, \beta^{\text{stick}})$  dynamic for Centipede of lengths  $d \in \{2, \dots, 20\}$ .  $p$  denotes the penultimate player,  $q$  the last player. The dashed lines separated exact ( $d \leq 6$ ) from numerical ( $d \geq 7$ ) results.

$p$	[7]	[6]	[5]	[4]	[3]	[2]	[1]	[0]
2	-	-	-	-	-	-	.585786	.414214
3	-	-	-	-	-	-	.598127	.401873
4	-	-	-	-	-	.187882	.589856	.222262
5	-	-	-	-	-	.268333	.511251	.220416
6	-	-	-	-	.029871	.380637	.412112	.177381
7	-	-	-	-	.059383	.367823	.396409	.176385
8	-	-	-	.000922	.115261	.342527	.374517	.166773
9	-	-	-	.002034	.119991	.340233	.371631	.166112
10	-	-	$1.43 \times 10^{-7}$	.004141	.119937	.339342	.370816	.165764
11	-	-	$2.88 \times 10^{-7}$	.004151	.119958	.339330	.370801	.165760
12	-	$1.15 \times 10^{-17}$	$5.76 \times 10^{-7}$	.004151	.119958	.339330	.370801	.165760
13	-	$2.31 \times 10^{-17}$	$5.76 \times 10^{-7}$	.004151	.119958	.339330	.370801	.165760
14	$4.26 \times 10^{-44}$	$4.62 \times 10^{-17}$	$5.76 \times 10^{-7}$	.004151	.119958	.339330	.370801	.165760
15	$8.53 \times 10^{-44}$	$4.62 \times 10^{-17}$	$5.76 \times 10^{-7}$	.004151	.119958	.339330	.370801	.165760
16	$1.71 \times 10^{-43}$	$4.62 \times 10^{-17}$	$5.76 \times 10^{-7}$	.004151	.119958	.339330	.370801	.165760
$\vdots$	$\vdots$	$\vdots$	$\vdots$	$\vdots$	$\vdots$	$\vdots$	$\vdots$	$\vdots$
20	$1.71 \times 10^{-43}$	$4.62 \times 10^{-17}$	$5.76 \times 10^{-7}$	.004151	.119958	.339330	.370801	.165760

$q$	[7]	[6]	[5]	[4]	[3]	[2]	[1]	[0]
2	-	-	-	-	-	-	.585786	.414214
3	-	-	-	-	-	.353505	.475030	.171464
4	-	-	-	-	-	.389143	.420433	.190425
5	-	-	-	-	.086214	.470163	.305175	.138448
6	-	-	-	-	.135659	.409203	.309724	.145414
7	-	-	-	.007525	.238377	.352249	.273400	.128450
8	-	-	-	.015754	.239929	.342189	.273010	.129117
9	-	-	$3.34 \times 10^{-5}$	.032755	.236217	.335328	.268586	.127081
10	-	-	$6.92 \times 10^{-5}$	.033304	.236208	.334871	.268485	.127063
11	-	$2.00 \times 10^{-11}$	.000139	.033311	.236192	.334839	.268465	.127053
12	-	$4.00 \times 10^{-11}$	.000139	.033311	.236192	.334839	.268465	.127053
13	$9.24 \times 10^{-28}$	$8.01 \times 10^{-11}$	.000139	.033311	.236192	.334839	.268465	.127053
14	$1.85 \times 10^{-27}$	$8.01 \times 10^{-11}$	.000139	.033311	.236192	.334839	.268465	.127053
15	$3.69 \times 10^{-27}$	$8.01 \times 10^{-11}$	.000139	.033311	.236192	.334839	.268465	.127053
$\vdots$	$\vdots$	$\vdots$	$\vdots$	$\vdots$	$\vdots$	$\vdots$	$\vdots$	$\vdots$
20	$3.69 \times 10^{-27}$	$8.01 \times 10^{-11}$	.000139	.033311	.236192	.334839	.268465	.127053

Table 9: The interior rest point of the  $\text{BEP}(\tau^{\text{adj}}, 1, \beta^{\text{unif}})$  dynamic for Centipede of lengths  $d \in \{2, \dots, 20\}$ .  $p$  denotes the penultimate player,  $q$  the last player. The dashed lines separated exact ( $d \leq 7$ ) from numerical ( $d \geq 8$ ) results.



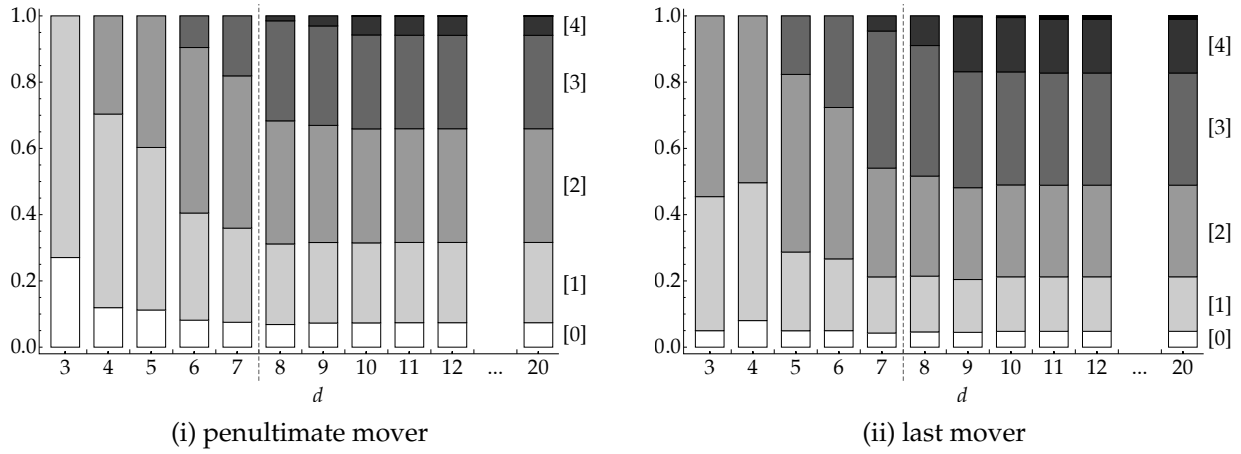


Figure 5: The stable rest point of Centipede under the  $\text{BEP}(\tau^{\text{adj}}, 1, \beta^{\min})$  dynamic for game lengths  $d = 3, \dots, 12$  and  $d = 20$ . Stacked bars, from the bottom to the top, represent weights on strategies [0], [1], [2], etc. The dashed line separates exact ( $d \leq 7$ ) and numerical ( $d \geq 8$ ) results.

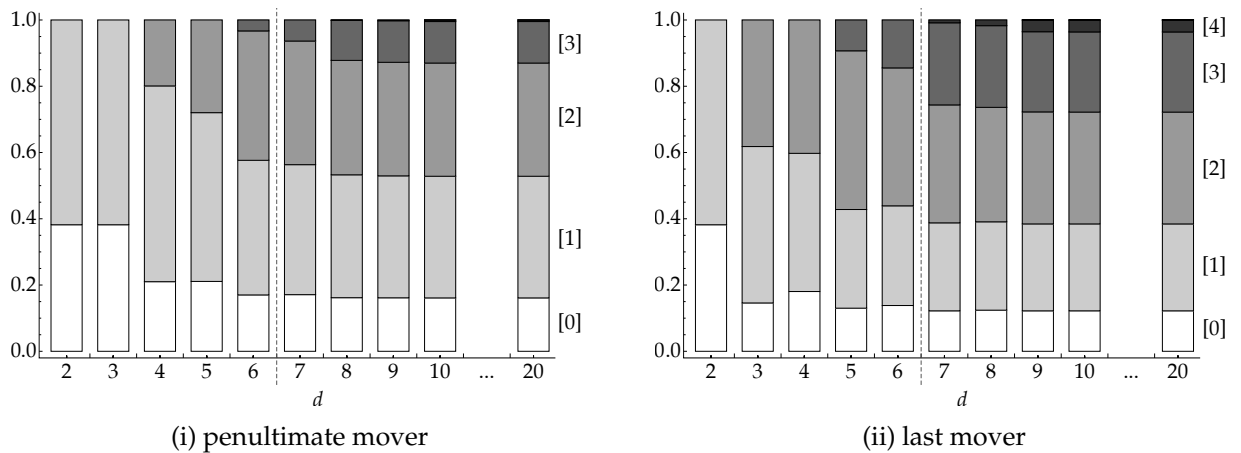


Figure 6: The stable rest point of Centipede under the  $\text{BEP}(\tau^{\text{adj}}, 1, \beta^{\text{stick}})$  dynamic for game lengths  $d = 3, \dots, 10$  and  $d = 20$ . Stacked bars, from the bottom to the top, represent weights on strategies [0], [1], [2], etc. The dashed line separates exact ( $d \leq 6$ ) and numerical ( $d \geq 7$ ) results.

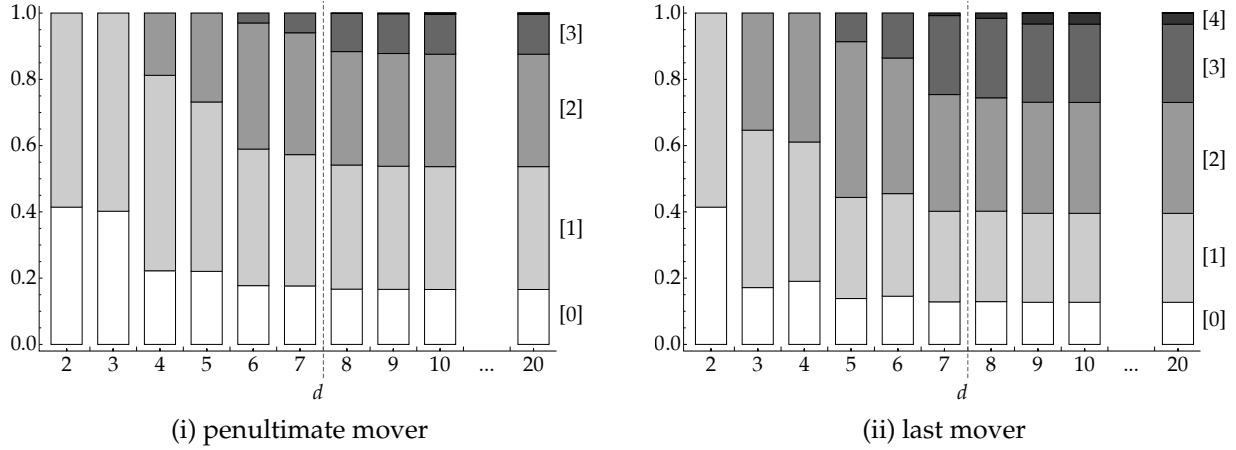


Figure 7: The stable rest point of Centipede under the  $\text{BEP}(\tau^{\text{adj}}, 1, \beta^{\text{unif}})$  dynamic for game lengths  $d = 3, \dots, 10$  and  $d = 20$ . Stacked bars, from the bottom to the top, represent weights on strategies [0], [1], [2], etc. The dashed line separates exact ( $d \leq 7$ ) and numerical ( $d \geq 8$ ) results.

## VI. Approximate eigenvalues of $DV(\xi^*)$ for $\text{BEP}(\tau, 1, \beta)$ dynamics

The tables in this section show approximate eigenvalues of the derivative matrix  $DV(\xi^*)$  at the interior rest point  $\xi^*$  of  $\text{BEP}(\tau, 1, \beta)$  dynamics in Centipede games of lengths up to  $d = 20$ . Tables 10, 11, and 12 present the approximate eigenvalues of  $DV(\xi^*)$  for the  $\text{BEP}(\tau^{\text{all}}, 1, \beta)$  dynamics with  $\beta = \beta^{\text{min}}, \beta^{\text{stick}},$  and  $\beta^{\text{unif}}$ . The approximate eigenvalues for  $\text{BEP}(\tau^{\text{two}}, 1, \beta)$  dynamics are in Tables 13–15, and those for  $\text{BEP}(\tau^{\text{adj}}, 1, \beta)$  dynamics are in Tables 16–18.

### VI.1 Test-all

$d = 3$	$-1 \pm .3820$	$-1$					
$d = 4$	$-1.1411 \pm .3277 i$	$-.8589 \pm .3277 i$					
$d = 5$	$-1.1355 \pm .3284 i$	$-.8645 \pm .3284 i$	$-1.$				
$d = 6$	$-1.1355 \pm .3284 i$	$-.8645 \pm .3284 i$	$-1. \pm 9.74 \times 10^{-5} i$				
$d = 7$	$-1.1355 \pm .3284 i$	$-.8645 \pm .3284 i$	$-1. \pm 9.74 \times 10^{-5} i$	$-1.$			
$d = 8$	$-1.1355 \pm .3284 i$	$-.8645 \pm .3284 i$	$-1. \pm 9.74 \times 10^{-5} i$	$-1.$	$-1.$		
$d = 9$	$-1.1355 \pm .3284 i$	$-.8645 \pm .3284 i$	$-1. \pm 9.74 \times 10^{-5} i$	$-1.$	$-1.$	$-1.$	
$d = 10$	$-1.1355 \pm .3284 i$	$-.8645 \pm .3284 i$	$-1. \pm 9.74 \times 10^{-5} i$	$-1.$	$-1.$	$-1.$	$\dots$
$\vdots$	$\vdots$	$\vdots$	$\vdots$	$\vdots$	$\vdots$	$\vdots$	$\dots$
$d = 20$	$-1.1355 \pm .3284 i$	$-.8645 \pm .3284 i$	$-1. \pm 9.74 \times 10^{-5} i$	$-1.$	$-1.$	$-1.$	$\dots$

Table 10: Approximate eigenvalues of  $DV(\xi^*)$  for the  $\text{BEP}(\tau^{\text{all}}, 1, \beta^{\text{min}})$  dynamic. The symbol “ $-1.$ ” is used as a shorthand for  $-1.0000$ .

$d = 2$	$-.8090 \pm .4468 i$							
$d = 3$	$-.9473 \pm .5843 i$	$-1$						
$d = 4$	$-1.2092 \pm .3992 i$	$-.7756 \pm .3807 i$						
$d = 5$	$-1.2134 \pm .3923 i$	$-.7732 \pm .3746 i$	$-.9989$					
$d = 6$	$-1.2134 \pm .3923 i$	$-.7732 \pm .3746 i$	$-.9989$	$-1.$				
$d = 7$	$-1.2134 \pm .3923 i$	$-.7732 \pm .3746 i$	$-.9989$	$-1.$	$-1.$			
$d = 8$	$-1.2134 \pm .3923 i$	$-.7732 \pm .3746 i$	$-.9989$	$-1.$	$-1.$	$-1.$		
$d = 9$	$-1.2134 \pm .3923 i$	$-.7732 \pm .3746 i$	$-.9989$	$-1.$	$-1.$	$-1.$	$\dots$	
$\vdots$	$\vdots$	$\vdots$	$\vdots$	$\vdots$	$\vdots$	$\vdots$	$\vdots$	$\dots$
$d = 20$	$-1.2134 \pm .3923 i$	$-.7732 \pm .3746 i$	$-.9989$	$-1.$	$-1.$	$-1.$	$\dots$	

Table 11: Approximate eigenvalues of  $DV(\xi^*)$  for the  $\text{BEP}(\tau^{\text{all}}, 1, \beta^{\text{stick}})$  dynamic. The symbol “-1.” is used as a shorthand for  $-1.0000$ .

$d = 2$	$-1 \pm .6436 i$							
$d = 3$	$-1 \pm .6353 i$	$-1$						
$d = 4$	$-1.2598 \pm .4255 i$	$-.7402 \pm .4255 i$						
$d = 5$	$-1.2602 \pm .4187 i$	$-.7398 \pm .4187 i$	$-1$					
$d = 6$	$-1.2602 \pm .4187 i$	$-.7398 \pm .4187 i$	$-1. \pm 7.94 \times 10^{-5} i$					
$d = 7$	$-1.2602 \pm .4187 i$	$-.7398 \pm .4187 i$	$-1. \pm 7.94 \times 10^{-5} i$	$-1.$				
$d = 8$	$-1.2602 \pm .4187 i$	$-.7398 \pm .4187 i$	$-1. \pm 7.94 \times 10^{-5} i$	$-1.$	$-1.$			
$d = 9$	$-1.2602 \pm .4187 i$	$-.7398 \pm .4187 i$	$-1. \pm 7.94 \times 10^{-5} i$	$-1.$	$-1.$	$-1.$		
$d = 10$	$-1.2602 \pm .4187 i$	$-.7398 \pm .4187 i$	$-1. \pm 7.94 \times 10^{-5} i$	$-1.$	$-1.$	$-1.$	$\dots$	
$\dots$	$\dots$	$\dots$	$\dots$	$\dots$	$\dots$	$\dots$	$\dots$	$\dots$
$d = 20$	$-1.2602 \pm .4187 i$	$-.7398 \pm .4187 i$	$-1. \pm 7.94 \times 10^{-5} i$	$-1.$	$-1.$	$-1.$	$\dots$	

Table 12: Approximate eigenvalues of  $DV(\xi^*)$  for the  $\text{BEP}(\tau^{\text{all}}, 1, \beta^{\text{unif}})$  dynamic. The symbol “-1.” is used as a shorthand for  $-1.0000$ .













## VII. Estimates of the basin of attraction of $\xi^+$ for $\text{BEP}(\tau^{\text{all}}, \kappa, \beta^{\text{min}})$ dynamics in Centipede of length $d = 4$

In this section, we provide estimates of the basin of attraction of the backward induction state  $\xi^+$  in Centipede games of length  $d = 4$  under  $\text{BEP}(\tau^{\text{all}}, \kappa, \beta^{\text{min}})$  dynamics. We do so for numbers of trials ranging from  $\kappa = 5$ , the smallest number for which  $\xi^+$  is asymptotically stable (see Proposition 6.1) to  $\kappa = 34$  and for selected larger values.

We estimated the size of the basin by numerically computing solutions to the  $\text{BEP}(\tau^{\text{all}}, \kappa, \beta^{\text{min}})$  dynamics from points in a grid of initial conditions of mesh  $\frac{1}{50}$  in the set of population states  $\Xi$ . This grid contains a total of  $\binom{52}{50}^2 = 1,758,276$  points, so an exhaustive exploration is not feasible. The algorithm we used to decide which points in the grid to explore aims at “growing” the basin of attraction from  $\xi^+$  outwards. Specifically, we start at the vertex  $\xi^+$  and extend outward, recursively visiting all neighboring points in the grid until obtaining a “boundary” two-grid-points thick in which no solution converges to  $\xi^+$ .

For  $\kappa \in \{5, \dots, 34\}$ , Table 19 presents all of the grid points from which solutions of  $\text{BEP}(\tau^{\text{all}}, \kappa, \beta^{\text{min}})$  dynamics converge to  $\xi^+$ . Table 20 presents the total number of such points, as well as the sum of the number of such points and the number of neighbors of such points; these numbers provide lower and upper bounds on the size of the basin.

We make two observations about these results. First, Table 19 shows that state  $\xi^+$  is not at all robust to changes in the behavior of population 1. This point is reinforced in Table 21, which shows that the saddle points of the dynamics all place mass of at least .998 on strategy 1. Second, Table 20 shows that the estimated size of the basin is very small. For instance, for  $\kappa = 100$ , the lower and upper estimates of the size of the basin are 51 and 166 grid points, out of the total of 1,758,276 grid points.

Condition on $\kappa$	$x_1$	$x_2$	$x_3$	$y_1$	$y_2$	$y_3$
	1	0	0	1	0	0
$\kappa \geq 6$	1	0	0	0.98	0.02	0
$\kappa = 7$ or $\kappa \geq 9$	1	0	0	0.96	0.04	0
$\kappa \geq 9$	1	0	0	0.94	0.06	0
$\kappa \geq 10$	1	0	0	0.98	0	0.02
$\kappa = 10$ or $\kappa \geq 12$	1	0	0	0.96	0.02	0.02
$\kappa = 10$ or $\kappa \geq 12$	1	0	0	0.92	0.08	0
$\kappa \geq 12$	1	0	0	0.94	0.04	0.02
$\kappa = 12, 13$ or $\kappa \geq 15$	1	0	0	0.9	0.1	0
$\kappa \geq 15$	1	0	0	0.92	0.06	0.02
$\kappa = 15, 16$ or $\kappa \geq 18$	1	0	0	0.88	0.12	0
$\kappa = 15, 16, 17, 18$ or $\kappa \geq 20$	1	0	0	0.96	0	0.04
$\kappa \geq 17$	1	0	0	0.9	0.08	0.02
$\kappa = 17$ or $\kappa \geq 20$	1	0	0	0.94	0.02	0.04
$\kappa = 18, 19$ or $\kappa \geq 21$	1	0	0	0.88	0.1	0.02
$\kappa = 18$ or $\kappa \geq 21$	1	0	0	0.86	0.14	0
$\kappa \geq 20$	1	0	0	0.92	0.04	0.04
$\kappa = 20$ or $\kappa \geq 25$	1	0	0	0.94	0	0.06
$\kappa = 21$ or $\kappa \geq 24$	1	0	0	0.86	0.12	0.02
$\kappa = 22$ or $\kappa \geq 24$	1	0	0	0.9	0.06	0.04
$\kappa = 24$ or $\kappa \geq 27$	1	0	0	0.84	0.16	0
$\kappa \geq 26$	1	0	0	0.88	0.08	0.04
$\kappa = 27$ or $\kappa \geq 30$	1	0	0	0.92	0.02	0.06
$\kappa = 27$ or $\kappa \geq 30$	1	0	0	0.84	0.14	0.02
$\kappa \geq 30$	1	0	0	0.86	0.1	0.04
$\kappa = 30$ or $\kappa \geq 33$	1	0	0	0.82	0.18	0
$\kappa \geq 32$	1	0	0	0.9	0.04	0.06
$\kappa = 33$	1	0	0	0.82	0.16	0.02

Table 19: Initial conditions in a grid of mesh  $\frac{1}{50}$  from which solutions of  $\text{BEP}(\tau^{\text{all}}, \kappa, \beta^{\text{min}})$  dynamics converge to  $\xi^\dagger$  ( $\kappa \in \{5, \dots, 34\}$ ).

$\kappa$	# in-basin points	# in-basin points and their out-of-basin neighbors
5	1	5
6	2	9
7	3	13
8	2	9
9	4	17
10	7	27
11	5	20
12	9	34
13	9	34
14	8	30
15	12	44
16	12	44
17	13	46
18	15	54
19	13	47
20	16	56
21	18	63
22	18	63
23	17	60
24	20	70
25	20	69
26	21	72
27	24	82
28	22	76
29	22	76
30	26	89
31	25	85
32	26	88
33	28	95
34	27	92
50	35	116
100	51	166

Table 20: Number of initial conditions in a grid of mesh  $\frac{1}{50}$  from which solutions of  $\text{BEP}(\tau^{\text{all}}, \kappa, \beta^{\text{min}})$  dynamics converge to  $\xi^+$ , and the total number of such points and their neighbors.

## VIII. Saddle points of $\text{BEP}(\tau^{\text{all}}, \kappa, \beta^{\text{min}})$ dynamics in Centipede of length $d = 4$

Table 21 presents approximate components of saddle points of  $\text{BEP}(\tau^{\text{all}}, \kappa, \beta^{\text{min}})$  dynamics for Centipede games of length  $d = 4$  for various  $\kappa$ .

	$x_1$	$x_2$	$x_3$		$y_1$	$y_2$	$y_3$
5	.999417	.000333	.000250	5	.994197	.002904	.002899
6	.999374	$8.23 \times 10^{-6}$	.000617	6	.992520	.003747	.003733
7	.999093	$6.76 \times 10^{-5}$	.000839	7	.987382	.006326	.006292
8	.999474	$3.20 \times 10^{-5}$	.000494	8	.991613	.004201	.004186
9	.999649	$1.93 \times 10^{-7}$	.000351	9	.993702	.003154	.003144
10	.998505	.000137	.001358	10	.970561	.014810	.014629
11	.998889	$9.75 \times 10^{-5}$	.001013	11	.975875	.012124	.012001
12	.998404	$4.76 \times 10^{-5}$	.001549	12	.962408	.018963	.018629
13	.998759	$3.35 \times 10^{-5}$	.001207	13	.968257	.015991	.015752
14	.998926	$3.65 \times 10^{-5}$	.001038	14	.970372	.014917	.014711
15	.998396	$3.72 \times 10^{-5}$	.001567	15	.953015	.023757	.023228
16	.998629	$3.45 \times 10^{-5}$	.001337	16	.957068	.021686	.021246
17	.998367	.000180	.001453	17	.946117	.027235	.026647
18	.998551	$1.69 \times 10^{-5}$	.001432	18	.949167	.025733	.025100
19	.998578	$3.19 \times 10^{-5}$	.001390	19	.947422	.026621	.025958
20	.998447	.000109	.001444	20	.939865	.030463	.029672
21	.998540	$1.58 \times 10^{-5}$	.001444	21	.940517	.030176	.029308
22	.998380	$6.61 \times 10^{-5}$	.001554	22	.931278	.034908	.033814
23	.998535	$6.48 \times 10^{-5}$	.001400	23	.934926	.033024	.032050
24	.998484	$2.03 \times 10^{-5}$	.001495	24	.929859	.035671	.034470
25	.998484	$4.05 \times 10^{-5}$	.001476	25	.927065	.037100	.035835
30	.998544	$1.69 \times 10^{-5}$	.001439	30	.916397	.042658	.040945
35	.998612	$4.21 \times 10^{-5}$	.001345	35	.907601	.047209	.045190
40	.998669	$2.03 \times 10^{-5}$	.001310	40	.899161	.051657	.049182
45	.998726	$1.04 \times 10^{-5}$	.001264	45	.891781	.055554	.052664
50	.998782	$2.29 \times 10^{-5}$	.001195	50	.885579	.058794	.055627
100	.999169	$2.75 \times 10^{-6}$	.000828	100	.847323	.079244	.073433
150	.999368	$5.23 \times 10^{-7}$	.000632	150	.827851	.089787	.082362
200	.999487	$2.93 \times 10^{-7}$	.000513	200	.815327	.096613	.088061

Table 21: Saddle points of  $\text{BEP}(\tau^{\text{all}}, \kappa, \beta^{\text{min}})$  dynamics for Centipede of length  $d = 4$ .

## IX. General formulation of best experienced payoff dynamics

In this appendix we use notation that allows us to describe protocols for both populations in a single expression. We denote the payoff matrices by  $U^1$  and  $U^2$ , and we write

population states as  $\xi = (\xi^1, \xi^2) \in \Xi = \Xi^1 \times \Xi^2$ , where  $\xi^p \in \Xi^p = \{\xi^p \in \mathbb{R}_+^{S^p} : \sum_{i \in S^p} \xi_i^p = 1\}$ .

We now define best experienced payoff revision protocols. Let  $\mathcal{P}(S^p)$  denote the power set of  $S^p$ . A *test-set distribution*  $\tau_i^p$  used by a strategy  $i \in S^p$  player is a probability distribution on  $\mathcal{P}(S^p)$  that places all of its mass on sets  $R^p \subseteq S^p$  that include strategy  $i$  and at least one other strategy. The *tie-breaking rule for strategy  $i \in S^p$* , denoted  $\beta_i^p$ , is a function that for each vector  $\pi^p$  of realized payoffs and each set of tested strategies  $R^p \subseteq S^p$  specifies the probability  $\beta_{ij}^p(\pi^p, R^p)$  of playing strategy  $j \in S^p$ . Since agents are payoff maximizers,  $\beta_{ij}^p(\pi^p, R^p)$  may only be positive if  $j \in \operatorname{argmax}_{k \in R^p} \pi_k^p$ . If there is a unique optimal strategy in  $R^p$ , it is chosen with probability one; in general,  $\beta_i^p(\pi^p, R^p)$  is a probability distribution on  $S^p$  whose support is contained in  $\operatorname{argmax}_{k \in R^p} \pi_k^p$ .

Now, given a collection  $(\tau, \kappa, \beta)$ , we define the corresponding *best experienced payoff protocol* as follows:

$$(16a) \quad \sigma_{ij}^p(U^p, \xi^q) = \sum_{R^p \subseteq S^p} \tau_i^p(R^p) \left[ \sum_r \left( \prod_{k \in R^p} \prod_{m=1}^{\kappa} \xi_{r_{km}}^q \right) \beta_{ij}^p(\pi^p(r), R^p) \right],$$

$$(16b) \quad \text{where } \pi_k^p(r) = \sum_{m=1}^{\kappa} U_{kr_{km}}^p \text{ for all } k \in R^p,$$

where  $U_{k\ell}^p$  denotes the payoff of a population  $p$  agent who plays  $k$  against an opponent playing  $\ell$ , and where the interior sum in (16a) is taken over all lists  $r: R^p \times \{1, \dots, \kappa\} \rightarrow S^q$  of the opponents' strategies during testing.

Inserting (16) into the mean dynamic equation from Section 2.2 yields the *best experienced payoff dynamic* defined by  $\tau$ ,  $\kappa$ , and  $\beta$ , called the *BEP*( $\tau, \kappa, \beta$ ) *dynamic* for short:

$$(17) \quad \dot{\xi}_i^p = \sum_{j \in S^p} \xi_j^p \left( \sum_{R^p \subseteq S^p} \tau_j^p(R^p) \left[ \sum_r \left( \prod_{k \in R^p} \prod_{m=1}^{\kappa} \xi_{r_{km}}^q \right) \beta_{ji}^p(\pi^p(r), R^p) \right] \right) - \xi_i^p,$$

with  $\pi^p(r)$  defined in (16b).

## X. Multinomial formulas for best experienced payoff dynamics

The general formula (B) for the *BEP*( $\tau, \kappa, \beta$ ) dynamic explicitly lists each of the  $\kappa$  strategies played an agent's opponents when an agent tests a strategy  $i$  in his test set. We can obtain a formula with far fewer terms by instead working with the *distribution* of opponents' strategies when the agent tests strategy  $i$ . Using such formulas is essential for numerical computations when  $\kappa$  is not small.

To express (B) in this form we introduce a number of definitions. Let

$$\mathbb{Z}_+^{s^q, \kappa} = \left\{ z \in \mathbb{Z}_+^{s^q} : \sum_{j \in S^q} z_j = \kappa \right\}$$

denote the set of possible (unnormalized) empirical distributions of opponents' strategies when a population  $p$  agent tests one of his own strategies  $\kappa$  times. When the state of population  $q$  is  $\xi^q \in \Xi^q$ , the probability that empirical distribution  $z$  occurs is the multinomial probability

$$M^{p, \kappa}(z, \xi^q) = \binom{\kappa}{z_1 \dots z_{s^q}} (\xi_1^q)^{z_1} \dots (\xi_{s^q}^q)^{z_{s^q}}.$$

And if a population  $p$  agent faces empirical distribution  $z$  when testing strategy  $i \in S^p$ , his total payoff is

$$\pi_i^p(z) = \sum_{j \in S^q} U_{ij}^p z_j.$$

Therefore, if we let  $\Pi_i^{p, \kappa}(\xi^q)$  be a random variable representing the total payoff obtained if strategy  $i \in S^p$  is tested  $\kappa$  times when the state of the opposing population is  $\xi^q$ , then the distribution of  $\Pi_i^{p, \kappa}(\xi^q)$  is

$$\mathbb{P}\left(\Pi_i^{p, \kappa}(\xi^q) = w_i^p\right) = \sum_{z \in \mathbb{Z}_+^{s^q, \kappa} : \pi_i^p(z) = w_i^p} M^{p, \kappa}(z, \xi^q).$$

We use the notation above to obtain our new expression for BEP dynamics. Let

$$W_i^{p, \kappa} = \{\pi_i^p(z) : z \in \mathbb{Z}_+^{s^q, \kappa}\}$$

denote the set of possible test results for strategy  $i \in S^p$  in  $\kappa$  trials. Also, for  $R^p \subseteq S^p$ , write  $W_{R^p}^{p, \kappa} = \prod_{k \in R^p} W_k^{p, \kappa}$ . Then we can express the BEP( $\tau, \kappa, \beta$ ) dynamic as

$$(18) \quad \dot{\xi}_i^p = \sum_{j \in S^p} \xi_j \left( \sum_{R^p \subseteq S^p} \tau_j^p(R^p) \left[ \sum_{w^p \in W_{R^p}^{p, \kappa}} \left( \prod_{k \in R^p} \mathbb{P}(\Pi_k^{p, \kappa}(\xi^q) = w_k^p) \right) \beta_{ji}^p(w^p, R^p) \right] \right) - \xi_i^p.$$

The general formula (18) becomes simpler if particular test-set and tie-breaking rules are chosen. For instance, under the convention that an empty product evaluates to 1, the BEP( $\tau^{\text{all}}, \kappa, \beta^{\text{min}}$ ) dynamic can be expressed as

$$\begin{aligned}\dot{x}_i &= \sum_{w_i^1 \in W_i^{1,\kappa}} \left( \mathbb{P}(\Pi_i^{1,\kappa}(y) = w_i^1) \prod_{k=1}^{i-1} \mathbb{P}(\Pi_k^{1,\kappa}(y) < w_i^1) \prod_{\ell=i+1}^{s^1} \mathbb{P}(\Pi_\ell^{1,\kappa}(y) \leq w_i^1) \right) - x_i, \\ \dot{y}_j &= \sum_{w_j^2 \in W_j^{2,\kappa}} \left( \mathbb{P}(\Pi_j^{2,\kappa}(x) = w_j^2) \prod_{k=1}^{j-1} \mathbb{P}(\Pi_k^{2,\kappa}(x) < w_j^2) \prod_{\ell=j+1}^{s^2} \mathbb{P}(\Pi_\ell^{2,\kappa}(x) \leq w_j^2) \right) - y_j.\end{aligned}$$

## XI. Formulas for $\text{BEP}(\tau, 1, \beta)$ dynamics in Centipede

This section provides explicit formulas for  $\text{BEP}(\tau, 1, \beta)$  dynamics in the Centipede game for the cases considered in the paper—that is, for  $\tau \in \{\tau^{\text{all}}, \tau^{\text{two}}, \tau^{\text{adj}}\}$  and  $\beta \in \{\beta^{\text{min}}, \beta^{\text{stick}}, \beta^{\text{unif}}\}$ . These are the formulas implemented in the `BEP_Centipede.nb` notebook.

### XI.1 Test-all

$\text{BEP}(\tau^{\text{all}}, 1, \beta^{\text{min}})$ :

$$\begin{aligned}\dot{x}_i &= \left( \sum_{k=i}^{s^2} y_k \right) \left( \sum_{m=1}^i y_m \right)^{s^1-i} + \sum_{k=2}^{i-1} y_k \left( \sum_{\ell=1}^{k-1} y_\ell \right)^{i-k} \left( \sum_{m=1}^k y_m \right)^{s^1-i} - x_i, \\ \dot{y}_j &= \begin{cases} \left( \sum_{k=2}^{s^1} x_k \right) (x_1 + x_2)^{s^2-1} + (x_1)^{s^2} - y_1 & \text{if } j = 1, \\ \left( \sum_{k=j+1}^{s^1} x_k \right) \left( \sum_{m=1}^{j+1} x_m \right)^{s^2-j} + \sum_{k=2}^j x_k \left( \sum_{\ell=1}^{k-1} x_\ell \right)^{j-k+1} \left( \sum_{m=1}^k x_m \right)^{s^2-j} - y_j & \text{otherwise.} \end{cases}\end{aligned}$$

$\text{BEP}(\tau^{\text{all}}, 1, \beta^{\text{stick}})$ :

$$\begin{aligned}
\dot{x}_i &= \binom{s^2}{k=i} \binom{i}{m=1}^{s^1-i} + \binom{i-1}{q=1} \sum_{k=2}^{i-1} y_k \binom{k-1}{\ell=1}^{i-k} \binom{k}{m=1}^{s^1-i} + \\
&+ \binom{s^1}{q=i+1} \sum_{k=2}^{i-1} y_k \binom{i-k-1}{\ell=1}^{i-k} \binom{k}{m=1}^{s^1-i-1} + \\
&+ x_i \sum_{k=2}^{i-1} y_k \binom{k-1}{\ell=1}^{i-k} \binom{k}{m=1}^{s^1-k-1} - x_i, \\
\dot{y}_j &= \binom{s^1}{k=j+1} \binom{j+1}{m=1}^{s^2-j} + \binom{j-1}{q=1} \sum_{k=2}^j x_k \binom{k-1}{\ell=1}^{j-k+1} \binom{k}{m=1}^{s^2-j} + \\
&+ \binom{s^2}{q=j+1} \sum_{k=2}^j x_k \binom{k-1}{\ell=1}^{j-k+2} \binom{k}{m=1}^{s^2-j-1} + \\
&+ y_j \left( (x_1)^{s^2} + \sum_{k=2}^j x_k \binom{k-1}{\ell=1} \binom{k}{m=1}^{s^2-k} \right) - y_j.
\end{aligned}$$



BEP( $\tau^{\text{all}}, 1, \beta^{\text{unif}}$ ):

$$\begin{aligned}\dot{x}_i &= \left( \sum_{j=i}^{s^2} y_j \right) \left( \sum_{j=1}^i y_j \right)^{s^1-i} + \sum_{k=2}^{i-1} y_k \left( \sum_{j=1}^{k-1} y_j \right)^{s^1-k-1} \sum_{j=0}^{s^1-k-1} \binom{s^1-k-1}{j} \frac{y_k^j}{j+1} \left( \sum_{\ell=1}^{k-1} y_\ell \right)^{s^1-k-1-j} - x_i, \\ \dot{y}_j &= \left( \sum_{h=j+1}^{s^1} x_h \right) \left( \sum_{h=1}^{j+1} x_h \right)^{s^2-j} + \frac{x_1^{s^2}}{s^2} + \sum_{k=2}^j x_k \left( \sum_{h=1}^{k-1} x_h \right)^{s^2-k} \sum_{h=0}^{s^2-k} \binom{s^2-k}{h} \frac{x_k^h}{h+1} \left( \sum_{\ell=1}^{k-1} x_\ell \right)^{s^2-k-h} - y_j.\end{aligned}$$

## XI.2 Test-two

BEP( $\tau^{\text{two}}, 1, \beta^{\text{min}}$ ):

$$\begin{aligned}\dot{x}_i &= \frac{1}{s^1-1} \sum_{h=1}^{i-1} \left[ \left( \sum_{k=h+1}^{s^2} y_k + \sum_{k=2}^h \sum_{\ell=1}^{k-1} y_k y_\ell \right) (x_i + x_h) \right] + \\ &+ \frac{1}{s^1-1} \sum_{h=i+1}^{s^1} \left[ \left( \sum_{k=i}^{s^2} \sum_{\ell=1}^i y_k y_\ell + \sum_{k=2}^{i-1} \sum_{\ell=1}^{k-1} y_k y_\ell + \sum_{k=1}^{i-1} y_k^2 \right) (x_i + x_h) \right] - x_i, \\ \dot{y}_j &= \frac{1}{s^2-1} \sum_{h=1}^{j-1} \left[ \left( \sum_{k=h+2}^{s^1} x_k + \sum_{k=2}^{h+1} \sum_{\ell=1}^{k-1} x_k x_\ell \right) (y_j + y_h) \right] + \\ &+ \frac{1}{s^2-1} \sum_{h=j+1}^{s^2} \left[ \left( \sum_{k=j+1}^{s^1} \sum_{\ell=1}^{j+1} x_k x_\ell + \sum_{k=2}^j \sum_{\ell=1}^{k-1} x_k x_\ell + \sum_{k=1}^j x_k^2 \right) (y_j + y_h) \right] - y_j.\end{aligned}$$

BEP( $\tau^{\text{two}}, 1, \beta^{\text{stick}}$ ):

$$\begin{aligned}\dot{x}_i &= \frac{1}{s^1-1} \sum_{h=1}^{i-1} \left[ \left( \sum_{k=h+1}^{s^2} y_k + \sum_{k=2}^h \sum_{\ell=1}^{k-1} y_k y_\ell \right) (x_i + x_h) + x_i \sum_{k=1}^{h-1} y_k^2 \right] + \\ &+ \frac{1}{s^1-1} \sum_{h=i+1}^{s^1} \left[ \left( \sum_{k=i}^{s^2} \sum_{\ell=1}^i y_k y_\ell + \sum_{k=2}^{i-1} \sum_{\ell=1}^{k-1} y_k y_\ell \right) (x_i + x_h) + x_i \sum_{k=1}^{i-1} y_k^2 \right] - x_i, \\ \dot{y}_j &= \frac{1}{s^2-1} \sum_{h=1}^{j-1} \left[ \left( \sum_{k=h+2}^{s^1} x_k + \sum_{k=2}^{h+1} \sum_{\ell=1}^{k-1} x_k x_\ell \right) (y_j + y_h) + y_j \sum_{k=1}^h x_k^2 \right] + \\ &+ \frac{1}{s^2-1} \sum_{h=j+1}^{s^2} \left[ \left( \sum_{k=j+1}^{s^1} \sum_{\ell=1}^{j+1} x_k x_\ell + \sum_{k=2}^j \sum_{\ell=1}^{k-1} x_k x_\ell \right) (y_j + y_h) + y_j \sum_{k=1}^j x_k^2 \right] - y_j.\end{aligned}$$

BEP( $\tau^{\text{two}}, 1, \beta^{\text{unif}}$ ):

$$\begin{aligned}
\dot{x}_i &= \frac{1}{s^1 - 1} \sum_{h=1}^{i-1} \left[ \left( \sum_{k=h+1}^{s^2} y_k + \sum_{k=2}^h \sum_{\ell=1}^{k-1} y_k y_\ell + \frac{1}{2} \sum_{k=1}^{h-1} y_k^2 \right) (x_i + x_h) \right] + \\
&+ \frac{1}{s^1 - 1} \sum_{h=i+1}^{s^1} \left[ \left( \sum_{k=i}^{s^2} \sum_{\ell=1}^i y_k y_\ell + \sum_{k=2}^{i-1} \sum_{\ell=1}^{k-1} y_k y_\ell + \frac{1}{2} \sum_{k=1}^{i-1} y_k^2 \right) (x_i + x_h) \right] - x_i, \\
\dot{y}_j &= \frac{1}{s^2 - 1} \sum_{h=1}^{j-1} \left[ \left( \sum_{k=h+2}^{s^1} x_k + \sum_{k=2}^{h+1} \sum_{\ell=1}^{k-1} x_k x_\ell + \frac{1}{2} \sum_{k=1}^h x_k^2 \right) (y_j + y_h) \right] + \\
&+ \frac{1}{s^2 - 1} \sum_{h=j+1}^{s^2} \left[ \left( \sum_{k=j+1}^{s^1} \sum_{\ell=1}^{j+1} x_k x_\ell + \sum_{k=2}^j \sum_{\ell=1}^{k-1} x_k x_\ell + \frac{1}{2} \sum_{k=1}^j x_k^2 \right) (y_j + y_h) \right] - y_j.
\end{aligned}$$

### XI.3 Test-adjacent

Let  $c_i^p$  equal 2 if  $i \in \{1, s^p\}$  and equal 1 otherwise, i.e.,  $c_i^p = 1 + \mathbf{1}[i \in \{1, s^p\}]$ .

BEP( $\tau^{\text{adj}}, 1, \beta^{\text{min}}$ ):

$$\begin{aligned}
\dot{x}_i &= \frac{1 - \mathbf{1}[i = 1]}{2} \sum_{h=i-1}^{i-1} \left[ \left( \sum_{k=h+1}^{s^2} y_k + \sum_{k=2}^h \sum_{\ell=1}^{k-1} y_k y_\ell \right) (c_i^1 x_i + c_h^1 x_h) \right] + \\
&+ \frac{1 - \mathbf{1}[i = s^1]}{2} \sum_{h=i+1}^{i+1} \left[ \left( \sum_{k=i}^{s^2} \sum_{\ell=1}^i y_k y_\ell + \sum_{k=2}^{i-1} \sum_{\ell=1}^{k-1} y_k y_\ell + \sum_{k=1}^{i-1} y_k^2 \right) (c_i^1 x_i + c_h^1 x_h) \right] - x_i, \\
\dot{y}_j &= \frac{1 - \mathbf{1}[j = 1]}{2} \sum_{h=j-1}^{j-1} \left[ \left( \sum_{k=h+2}^{s^1} x_k + \sum_{k=2}^{h+1} \sum_{\ell=1}^{k-1} x_k x_\ell \right) (c_j^2 y_j + c_h^2 y_h) \right] + \\
&+ \frac{1 - \mathbf{1}[j = s^2]}{2} \sum_{h=j+1}^{j+1} \left[ \left( \sum_{k=j+1}^{s^1} \sum_{\ell=1}^{j+1} x_k x_\ell + \sum_{k=2}^j \sum_{\ell=1}^{k-1} x_k x_\ell + \sum_{k=1}^j x_k^2 \right) (c_j^2 y_j + c_h^2 y_h) \right] - y_j.
\end{aligned}$$

BEP( $\tau^{\text{adj}}, 1, \beta^{\text{stick}}$ ):

$$\begin{aligned}
\dot{x}_i &= \frac{1 - \mathbf{1}[i = 1]}{2} \sum_{h=i-1}^{i-1} \left[ \left( \sum_{k=h+1}^{s^2} y_k + \sum_{k=2}^h \sum_{\ell=1}^{k-1} y_k y_\ell \right) (c_i^1 x_i + c_h^1 x_h) + c_i^1 x_i \sum_{k=1}^{h-1} y_k^2 \right] + \\
&+ \frac{1 - \mathbf{1}[i = s^1]}{2} \sum_{h=i+1}^{i+1} \left[ \left( \sum_{k=i}^{s^2} \sum_{\ell=1}^i y_k y_\ell + \sum_{k=2}^{i-1} \sum_{\ell=1}^{k-1} y_k y_\ell \right) (c_i^1 x_i + c_h^1 x_h) + c_i^1 x_i \sum_{k=1}^{i-1} y_k^2 \right] - x_i, \\
\dot{y}_j &= \frac{1 - \mathbf{1}[j = 1]}{2} \sum_{h=j-1}^{j-1} \left[ \left( \sum_{k=h+2}^{s^1} x_k + \sum_{k=2}^{h+1} \sum_{\ell=1}^{k-1} x_k x_\ell \right) (c_j^2 y_j + c_h^2 y_h) + c_j^2 y_j \sum_{k=1}^h x_k^2 \right] + \\
&+ \frac{1 - \mathbf{1}[j = s^2]}{2} \sum_{h=j+1}^{j+1} \left[ \left( \sum_{k=j+1}^{s^1} \sum_{\ell=1}^{j+1} x_k x_\ell + \sum_{k=2}^j \sum_{\ell=1}^{k-1} x_k x_\ell \right) (c_j^2 y_j + c_h^2 y_h) + c_j^2 y_j \sum_{k=1}^j x_k^2 \right] - y_j.
\end{aligned}$$

BEP( $\tau^{\text{adj}}, 1, \beta^{\text{unif}}$ ):

$$\begin{aligned}
\dot{x}_i &= \frac{1 - \mathbf{1}[i = 1]}{2} \sum_{h=i-1}^{i-1} \left[ \left( \sum_{k=h+1}^{s^2} y_k + \sum_{k=2}^h \sum_{\ell=1}^{k-1} y_k y_\ell + \frac{1}{2} \sum_{k=1}^{h-1} y_k^2 \right) (c_i^1 x_i + c_h^1 x_h) \right] + \\
&+ \frac{1 - \mathbf{1}[i = s^1]}{2} \sum_{h=i+1}^{i+1} \left[ \left( \sum_{k=i}^{s^2} \sum_{\ell=1}^i y_k y_\ell + \sum_{k=2}^{i-1} \sum_{\ell=1}^{k-1} y_k y_\ell + \frac{1}{2} \sum_{k=1}^{i-1} y_k^2 \right) (c_i^1 x_i + c_h^1 x_h) \right] - x_i, \\
\dot{y}_j &= \frac{1 - \mathbf{1}[j = 1]}{2} \sum_{h=j-1}^{j-1} \left[ \left( \sum_{k=h+2}^{s^1} x_k + \sum_{k=2}^{h+1} \sum_{\ell=1}^{k-1} x_k x_\ell + \frac{1}{2} \sum_{k=1}^h x_k^2 \right) (c_j^2 y_j + c_h^2 y_h) \right] + \\
&+ \frac{1 - \mathbf{1}[j = s^2]}{2} \sum_{h=j+1}^{j+1} \left[ \left( \sum_{k=j+1}^{s^1} \sum_{\ell=1}^{j+1} x_k x_\ell + \sum_{k=2}^j \sum_{\ell=1}^{k-1} x_k x_\ell + \frac{1}{2} \sum_{k=1}^j x_k^2 \right) (c_j^2 y_j + c_h^2 y_h) \right] - y_j.
\end{aligned}$$

## References

- Akritis, A. G. (2010). Vincent's theorem of 1836: Overview and future research. *Journal of Mathematical Sciences*, 168:309–325.
- Akritis, A. G., Bocharov, A., and Strzeboński, A. W. (1994). Implementation of real root isolation algorithms in *Mathematica*. In *Abstracts of the International Conference on Interval and Computer-Algebraic Methods in Science and Engineering (Interval '94)*, pages 23–27, St. Petersburg.
- Alefeld, G. and Herzberger, J. (1983). *Introduction to Interval Computations*. Academic Press, New York.

- Buchberger, B. (1965). *Ein Algorithmus zum Auffinden der Basiselemente des Restklassenrings nach einem nulldimensionalen Polynomideal*. PhD thesis, University of Innsbruck. Translated by M.P. Abramson as “An algorithm for finding the basis elements of the residue class ring of a zero-dimensional polynomial ideal” in *Journal of Symbolic Computation* 41 (2006), 475–511.
- Buchberger, B. (1970). Ein algorithmisches Kriterium für die Lösbarkeit eines algebraischen Gleichungssystems. *Aequationes mathematicae*, pages 374–383. Translated by M. P. Abramson and R. Lumbert as “An algorithmic criterion for the solvability of algebraic systems of equations” in B. Buchberger and F. Winkler, editors, *Gröbner Bases and Applications*, p. 535–545, 1998, Cambridge University Press.
- Collins, G. E. (1975). Quantifier elimination for the theory of real closed fields by cylindrical algebraic decomposition. In *Second GI Conference on Automata Theory and Formal Languages*, volume 33 of *Lecture Notes in Computer Science*, pages 134–183. Springer, Berlin.
- Collins, G. E. and Krandick, W. (1992). An efficient algorithm for infallible polynomial complex root isolation. In Wang, P. S., editor, *Proceedings of the International Symposium on Symbolic and Algebraic Computation (ISSAC '92)*, pages 189–194, Berkeley.
- Cox, D., Little, J., and O’Shea, D. (2015). *Ideals, Varieties, and Algorithms: An Introduction to Computational Algebraic Geometry and Commutative Algebra*. Springer International, Cham, Switzerland, fourth edition.
- Guggenheimer, H. W., Edelman, A. S., and Johnson, C. R. (1995). A simple estimate of the condition number of a linear system. *College Mathematics Journal*, 26:2–5.
- Jenkins, M. A. (1969). *Three-stage variable-shift iterations for the solution of polynomial equations with a posteriori error bounds for the zeros*. PhD thesis, Stanford University.
- Jenkins, M. A. and Traub, J. F. (1970a). A three-stage algorithm for real polynomials using quadratic iteration. *SIAM Journal on Numerical Analysis*, 7:545–566.
- Jenkins, M. A. and Traub, J. F. (1970b). A three-stage variable-shift iteration for polynomial zeros and its relation to generalized Rayleigh iteration. *Numerische Mathematik*, 14:252–263.
- Sandholm, W. H. (2007). Evolution in Bayesian games II: Stability of purified equilibria. *Journal of Economic Theory*, 136:641–667.
- Strzeboński, A. W. (1996). Algebraic numbers in *Mathematica 3.0*. *Mathematica Journal*, 6:74–80.
- Strzeboński, A. W. (1997). Computing in the field of complex algebraic numbers. *Journal of Symbolic Computation*, 24:647–656.
- Tucker, W. (2011). *Validated Numerics: A Short Introduction to Rigorous Computations*. Princeton University Press, Princeton.